The pulmonary vasculature in lethal COVID-19 and idiopathic pulmonary fibrosis at single cell resolution

Laura P.M.H. de Rooij[1#], Lisa M. Becker[1#], Laure-Anne Teuwen[1], Bram Boeckx[2], Sander Jansen[3], Simon Feys[4], Stijn Verleden[5^], Laurens Liesenborghs[3], Anna K. Stalder[6] Sasha Libbrecht[7], Tina Van Buyten[3], Gino Philips[2], Abhishek Subramanian[1], Sébastien J. Dumas[1], Elda Meta[1], Mila Borri[1], Liliana Sokol[1], Amélie Dendooven[7,8], Anh-Co K. Truong[1], Jan Gunst[9], Pierre Van Mol[2], Jasmin D. Haslbauer[20], Katerina Rohlenova[1§], Thomas Menter[6], Robbert Boudewijns[3], Vincent Geldhof[1], Stefan Vinckier[1], Jacob Amersfoort[1], Wim Wuyts[10], Dirk Van Raemdonck[5], Werner Jacobs[11], Laurens J. Ceulemans[5], Birgit Weynand[12], Bernard Thienpont[13], Martin Lammens[14,15], Mark Kuehnel[16,17], Guy Eelen[1], Mieke Dewerchin[1], Luc Schoonjans[1,2], Danny Jonigk[16,17], Jo van Dorpe[7], Alexandar Tzankov[6], Els Wauters[5,18], Massimiliano Mazzone[19,20], Johan Neyts[3], Joost Wauters[4], Diether Lambrechts[2] & Peter Carmeliet[1,21,22&]*

(1) Laboratory of Angiogenesis and Vascular Metabolism, Department of Oncology and Leuven Cancer Institute (LKI), KU Leuven, VIB Center for Cancer Biology, VIB, Leuven 3000, Belgium; (2) Laboratory of Translational Genetics, Center for Cancer Biology, VIB & Department of Genetics, KU Leuven, Leuven 3000, Belgium; (3) Laboratory of Virology & Chemotherapy, KU Leuven, Leuven, Belgium; (4) Medical Intensive Care Unit, UZ Gasthuisberg & Laboratory for Clinical Infectious and Inflammatory Disorders, Department of Microbiology, Immunology and Transplantation, KU Leuven, B-3000 Leuven, Belgium; (5) Laboratory of Respiratory Diseases and Thoracic Surgery (BREATHE), KU Leuven, Leuven, 3000, Belgium; (6) Institute of Medical Genetics and Pathology, University Hospital Basel, Basel, Switzerland; (7) Department of Pathology, Ghent University Hospital, Ghent University, Ghent, Belgium; (8) University of Antwerp, Faculty of Medicine, Wilrijk, Belgium; (9) Laboratory of Intensive Care Medicine, Department of Cellular and Molecular Medicine, KU Leuven, Leuven, 3000, Belgium; (10) Department of Respiratory Medicine, Unit for Interstitial Lung Diseases, UZ Gasthuisberg, Leuven, Belgium; (11) Medical CBRNe unit, Queen Astrid Military Hospital, Belgian Defense, Nederoverheembeek 1120, Belgium & Department of Forensic Pathology, ASTARC Antwerp University Hospital and University of Antwerp, Antwerp 2610, Belgium; (12) Translational Cell & Tissue Research, Department of Imaging & Pathology, KU Leuven, Leuven, Belgium; (13) Laboratory for Functional Epigenetics, Department of Human Genetics, KU Leuven, 3000 Leuven, Belgium;

© The Author(s) 2022. Published by Oxford University Press on behalf of European Society of Cardiology. This is an Open Access article distributed under the terms of the Creative Commons Attribution-NonCommercial License (https://creativecommons.org/licenses/by-nc/4.0/), which permits non-commercial re-use, distribution, and reproduction in any medium, provided the original work is properly cited. For commercial re-use, please contact journals.permissions@oup.com

ACCEPTED MANUSCRIPT

(14) Department of Pathology Antwerp University Hospital, Edegem 2560, Belgium; (15) Center for Oncological Research, University of Antwerp, Antwerp 2000, Belgium; (16) Medizinische Hochschule Hannover (MHH), Institut für Pathologie, D-30625 Hannover; (17) Biomedical Research in Endstage and Obstructive Lung Disease Hannover (BREATH) Member of the German Centre for Lung research (DZL), Hannover, Germany; (18) Respiratory Oncology Unit, University Hospital KU Leuven, Leuven, Belgium; (19) Laboratory of Tumor Inflammation and Angiogenesis, Center for Cancer Biology, VIB, Leuven 3000, Belgium; (20) Laboratory of Tumor Inflammation and Angiogenesis, Center for Cancer Biology, Department of Oncology, KU Leuven, Leuven 3000, Belgium. (21) Laboratory of Angiogenesis and Vascular Heterogeneity, Department of Biomedicine, Aarhus University, Aarhus 8000, Denmark. (22) Center for Biotechnology, Khalifa University of Science and Technology, Abu Dhabi, United Arab Emirates. *current address: Department of Oncology, Antwerp University Hospital (UZA), Edegem 2650, Belgium; §current address: Institute of Biotechnology, Czech Academy of Sciences, BIOCEV, Vestec 252 50, Czech Republic. ˆcurrent address: Department of Antwerp Surgical Training, Anatomy and Research Centre, division of thoracic and vascular Surgery. University of Antwerp, Wilrijk, Belgium.

#: contribute equally

&: Lead contact

Editorial correspondence: Peter Carmeliet, M.D., Ph.D. (lead contact); peter.carmeliet@kuleuven.be

KEY WORDS: SARS-CoV-2; COVID-19; IPF; transcriptomics; single nucleus RNA-seq; lung; endothelial cells

ACCEPTED MANUSCRIPT

ABSTRACT

Aims: SARS-CoV-2 infection causes COVID-19, which in severe cases evokes life-threatening acute respiratory distress syndrome (ARDS). Transcriptome signatures and the functional relevance of non-vascular cell types (e.g. immune and epithelial cells) in COVID-19 are becoming increasingly evident. However, despite its known contribution to vascular inflammation, recruitment/invasion of immune cells, vascular leakage and perturbed hemostasis in the lungs of severe COVID-19 patients, an in-depth interrogation of the endothelial cell (EC) compartment in lethal COVID-19 is lacking. Moreover, progressive fibrotic lung disease represents one of the complications of COVID-19 pneumonia and ARDS. Analogous features between idiopathic pulmonary fibrosis (IPF) and COVID-19 suggest partial similarities in their pathophysiology, yet, a head-to-head comparison of pulmonary cell transcriptomes between both conditions has not been implemented to date.

Methods and Results: We performed single nucleus RNA-seq (snRNA-seq) on frozen lungs from 7 deceased COVID-19 patients, 6 IPF explant lungs and 12 controls. The vascular fraction, comprising 38,794 nuclei, could be subclustered into 14 distinct EC subtypes. Non-vascular cell types, comprising 137,746 nuclei, were subclustered and used for EC-interactome analyses. Pulmonary ECs of deceased COVID-19 patients showed an enrichment of genes involved in cellular stress, as well as signatures suggestive of dampened immunomodulation and impaired vessel wall integrity. In addition, increased abundance of a population of systemic capillary and venous ECs was identified in COVID-19 and IPF. COVID-19 systemic ECs closely resembled their IPF counterparts, and a set of 30 genes was found congruently enriched in systemic ECs across studies. Receptor-ligand interaction analysis of ECs with non-vascular cell types in the pulmonary micro-environment revealed numerous previously unknown interactions specifically enriched/depleted in COVID-19 and/or IPF.

Conclusions: This study uncovered novel insights into the abundance, expression patterns and interactomes of EC subtypes in COVID-19 and IPF, relevant for future investigations into the progression and treatment of both lethal conditions.

ACCEPTED MANUSCRIPT

Translational perspective: While assessing clinical and molecular characteristics of severe and lethal COVID-19 cases, the vasculature's undeniable role in disease progression has been widely acknowledged. COVID-19 lung pathology moreover shares certain clinical features with late-stage IPF – yet an in-depth interrogation and direct comparison of the endothelium at single-cell level in both conditions is still lacking. By comparing the transcriptomes of ECs from lungs of deceased COVID-19 patients to those from IPF explant and control lungs, we gathered key insights the heterogeneous composition and potential roles of ECs in both lethal diseases, which may serve as a foundation for development of novel therapeutics.

ACCEPTED MANUSCRIPT

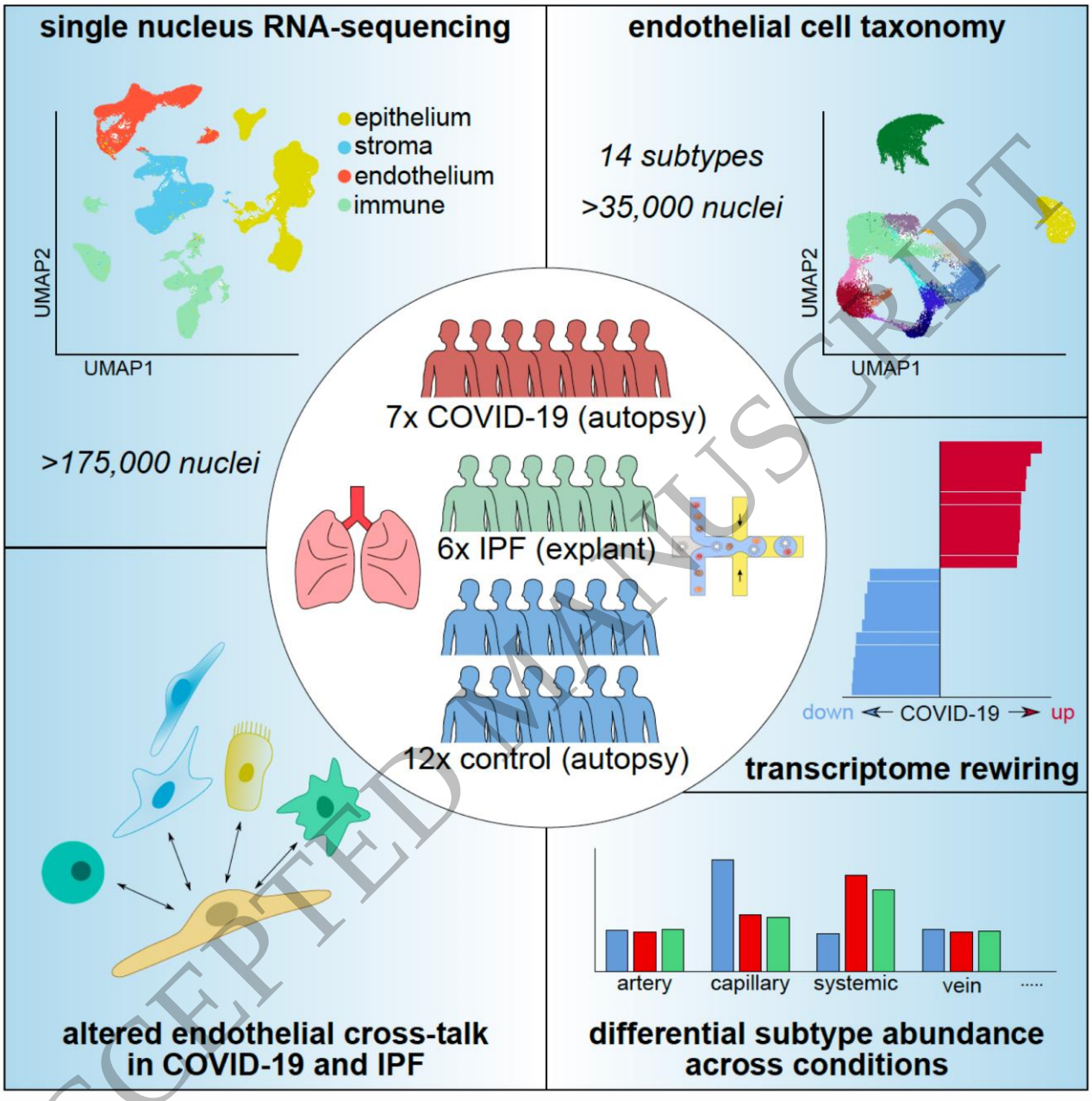

Graphical Abstract

ACCEPTED MANUSCRIPT

INTRODUCTION

The pandemic caused by severe acute respiratory syndrome coronavirus 2 (SARS-CoV-2) continues to progress and flare up. COVID-19, caused by SARS-CoV-2 infection, manifests as acute respiratory distress syndrome (ARDS)[1] in severe cases, too often with life-threatening consequences. Despite ongoing vaccination programs and therapeutic improvements[2,3], mortality of a fraction of acutely-ill severe COVID-19 patients and chronic morbidity of severe COVID-19 survivors remain unacceptably high, and SARS-CoV-2 mutants continue to threaten healthcare, economic welfare and quality of life in multiple countries. As single-cell studies provide an unbiased and comprehensive characterization of cellular landscapes, they represent a suitable strategy for increasing our understanding of the cell phenotypes and transcriptomic underpinnings of COVID-19. Previous single-cell studies profiled the response to SARS-CoV-2 in peripheral blood mononuclear cells (PBMCs) and bronchoalveolar lavage fluid (BALF), primarily focusing on immune cells[4-12]. Subsequent single-cell studies then also compiled inventories of the pulmonary cell heterogeneity in organs from deceased COVID-19 patients ("lethal COVID-19")[13-15].

Endothelial cells (ECs) have been proposed to contribute to vascular inflammation, recruitment/invasion of immune cells, vascular leakage, hypercoagulability, vascular thrombotic occlusion and resultant hypoxia in the lungs of severe COVID-19 patients[16-19]. Moreover, non-vascular cells, in particular immune cells, in the pulmonary micro-environment can render ECs dysfunctional[20]. Nevertheless, the vascular landscape, as well as its interplay with non-vascular cells, remains underexplored at in-depth single-cell resolution in COVID-19.

Important to consider when interrogating the lung vasculature, the lung harbors two circulatory systems: the pulmonary circulation, important for gas exchange, and the systemic/bronchial vascular supply, providing oxygenated blood to the entire lung[21]. In fact, in addition to the more established pulmonary EC subtypes, so-called peri-bronchial venous ECs were identified as a transcriptomically distinct vascular subcluster in a single-cell RNA-sequencing (scRNA-

ACCEPTED MANUSCRIPT

seq) study of lungs from healthy, idiopathic pulmonary fibrosis (IPF; a lung disease characterized by progressive lung scarring and irreversible lung dysfunction) and chronic obstructive pulmonary disease (COPD) patients[22]. In healthy lungs, this EC subtype is restricted to the bronchial vasculature surrounding large proximal airways, while in IPF lungs, peri-bronchial venous ECs expand and are observed in areas of bronchiolization and fibrosis[22]. In subsequent lung EC scRNA-seq studies, this EC subtype was specifically localized to the systemic vasculature of the bronchial vascular plexus and visceral pleura in healthy lungs, and ultimately coined as 'systemic venous'[15,23].

IPF shares a number of major risk factors and molecular characteristics with COVID-19[24-26], and patients with COVID-19 associated ARDS often develop severe pulmonary fibrosis[27,28], which can be life-threatening in the acute stage and often results in incapacitating sequelae later on[29]. A population of systemic venous ECs has also been recently detected in COVID-19 lungs[15], but its putative role in fibrotic lung disease, as well as additional heterogeneity within this EC subpopulation, either within or between conditions, remains elusive to date.

Since a direct comparison of COVID-19- vs. non-COVID-19-related pulmonary fibrosis has not been conducted to date, we performed a single-nucleus RNA-sequencing (snRNA-seq) study on frozen lung tissue from 7 COVID-19 decedents, 6 IPF patients (who required lung transplantation) and 12 controls (for detailed patient information, see Supplementary Methods and Table S1), and derived transcriptomes of 38,794 single ECs, distributed over 14 distinct subclusters. Whereas COVID-19 and IPF samples largely resembled each other in terms of subcluster distribution and differentially expressed genes, we detected notable differences in transcriptome signatures and subcluster abundances when comparing both conditions to control lungs, including an increased abundance of systemic venous, and newly discovered systemic capillary ECs in both COVID-19 and IPF lungs. By taking advantage of the 137,746 nuclei of non-vascular cell types, we performed EC-interactome analyses and identified a perturbed crosstalk between vascular and non-vascular compartments in lethal COVID-19. We moreover identified a congruent set of 30 genes, selectively enriched in systemic ECs across multiple COVID-19 and IPF studies, comprising different patient cohorts and sequencing

ACCEPTED MANUSCRIPT

strategies. Altogether, we highlight key transcriptomic changes and interactions perturbed in COVID-19 with focus on the endothelium, partially overlapping with IPF, and with potential importance for future therapeutic development.

METHODS

PATIENT SAMPLES

Informed consent was obtained from all research subjects. Sample collection and use were approved by the local ethics committee (Medical Ethics Committee UZ/KU Leuven, see Supplementary Methods for specific ethical protocols). The study complied with the principles outlined in the Declaration of Helsinki. All SARS-CoV-2-positive samples were handled and processed in a biosafety level-3 laboratory, according to the biocontainment procedures associated with processing of SARS-CoV-2-positive samples. For more detailed patient information see Supplementary Methods and Table S1. All Non-COVID-19 control patient tissues were collected before the 2020 pandemic, and therefore SARS-CoV-2 negative.

SINGLE NUCLEI ISOLATION FROM CONTROL, COVID-19 AND IPF LUNG TISSUES

For snRNA-seq, after collection, freezing of lung post-mortem/explant samples was performed as quickly as possible by placing the samples in cryo-tubes, which were subsequently snap-frozen with liquid N2 (5 min). Afterwards, the tubes were placed on dry ice and stored at -80°C. The nuclei isolation protocol was adapted from[30] (see Supplementary Methods for more details).

SNRNA-SEQ

Nuclei were counted using an automated cell counter (Luna, Logos Biosystems), and converted to barcoded Drop-seq libraries by using the Chromium Single 3' Library, Gel Bead & Multiplex Kit and Chip Kit (10X Genomics; Pleasanton, California, USA), aiming for an estimated number of 10,000 nuclei per library. Libraries were sequenced on an Illumina NovaSeq 6000. Demultiplexing according to the sample barcodes, and subsequent read alignment were done using Cell Ranger (v3.1.0). A

ACCEPTED MANUSCRIPT

human reference genome (GRCh38) was used, including intron sequences for mapping of reads obtained from snRNA-seq data. Three Fastq files were generated per sample: The I1 Fastq contains the sample barcode, R1 Fastq contains the cell barcode and UMI, and the R2 Fastq contains the cDNA (88nt).

SNRNA-SEQ DATA ANALYSIS

After generation of the gene expression matrices, raw data was processed further in R (version 4.0.1). The following quality control steps were performed: (i) genes expressed by less than 10 nuclei were removed; (ii) nuclei that expressed fewer than 250 genes (low quality), and with a detected number of genes > 2 standard deviations above the mean (potential doublets) were excluded from further analysis; (iii) nuclei with a detected fraction of mitochondrial genes >20% were removed. The resulting data (259,297 nuclei) was first normalized using the *NormalizeData* function as implemented in the *Seurat* package (v3.1). We next identified the top-2000 highly variable genes (*FindVariableFeatures* function), followed by scaling of the data (*ScaleData* function). The data were then summarized by principal component analysis (PCA; *RunPCA* function). The top 35 PCs were used to construct a shared nearest-neighbor graph (SNN; *FindNeighbors* function) used to cluster the dataset (*FindClusters* function, resolution = 0.5), followed by visualization using uniform manifold approximation and projection (UMAP; *runUMAP* function). Marker genes for each cluster were calculated using *FindAllMarkers(),* and clusters were annotated and subsetted (using the *subset()* function) into major cellular lineages based on the expression of canonical marker genes, including *PECAM1* and *CDH5* for ECs, *COL1A1, ACTA2, DCN* and *LUM* for stromal cells, *EPCAM* and *SFTPC* for epithelial cells, and *PTPRC* for immune cells (which could be further divided into NK/T cells (*CD3E, NKG7*), myeloid cells (*MARCO, CD163, FCN1*), B cells (*MS4A1*), mast cells (*MS4A2, KIT*), plasma cells (*JCHAIN*)). Individual subclustering was then performed for the epithelial, stromal, immune (NK/T and myeloid subsets only) and endothelial subsets (See Supplementary Methods for further details).

ACCEPTED MANUSCRIPT

HISTOLOGICAL AND IMMUNOHISTOCHEMICAL ANALYSIS

See Supplementary Methods.

QUANTIFICATION AND STATISTICAL ANALYSIS

Statistical analyses were performed using GraphPad Prism (GraphPad Software, USA). Comparison of changes between two groups was performed using an unpaired, two-tailed t-test (in case of normally distributed data, as determined by performing a Shapiro-Wilk test) or a Mann-Whitney test (unpaired; two-tailed; in case data was not normally distributed). In case of unequal variance (F-test), a Welch t-test was used. Comparison of changes between multiple groups was performed using a Kruskal-Wallis test and Dunn's test for multiple comparisons. All immunofluorescence- or histochemical analyses were repeated in a minimum of 3 patients per group and representative images are displayed.

RESULTS

ATLAS OF PULMONARY SUBTYPES IN LETHAL COVID-19 AND IPF

The goal of this study was to analyze pulmonary cell transcriptomic heterogeneity in lethal COVID-19 at cellular resolution, and to compare it to the single-cell transcriptome signature of IPF. To as much as possible avoid confounding study design differences introduced by comparing existing datasets of COVID-19 and IPF lung tissues, we compared head-to-head both lung diseases in a single study, by performing snRNA-seq on frozen lung tissues from 7 COVID-19 decedents, 6 IPF patients requiring lung transplantation, and 12 controls who died of causes unrelated to lung disease (Figure 1A, for clinical metadata see Table S1).

We profiled a total of 176,540 nuclei, distributed over different cellular lineages, detected in every sample and condition: ECs (*PECAM1*), stromal cells (defined as a mix of fibroblasts (*COL1A2*, *FN1*), pericytes (*PDGFRB*) and smooth muscle cells (*ACTA2*), according to a previously published lung taxonomy[31]), epithelial cells (*EMP2*, *EPCAM*), and immune cells (mix of myeloid cell types (*MRC1, ITGAX, FCN1*), T cells (*CD3E*), NK cells (*NKG7*), B cells (*MS4A1*), mast cells (*MS4A2*) and plasma cells

ACCEPTED MANUSCRIPT

(*JCHAIN*)) (Fig. 1A,B; Figure S1A; Table S2). Epithelial cells were underrepresented in lethal COVID-19 lungs, whereas stromal cells were enriched (Figure 1C,D), a finding corroborated by immunostaining for the epithelial marker cytokeratin-7 (CK7) (Figure 1E), and the stromal cell marker alpha-smooth muscle actin (αSMA) (Figure 1F), in line with previous findings[15]. Similar trends were observed in IPF, as previously reported[22,32-34]. Further sub-clustering of the different cellular lineages revealed 61 subclusters (Fig. 1G), in line with reported single-cell human lung taxonomies[22,31,35,36], and detected in all three conditions.

PHENOTYPIC HETEROGENEITY OF ECS IN COVID-19, IPF AND CONTROL LUNG TISSUE

Given the increasing availability of single-cell analyses of non-vascular cell types in COVID-19 and IPF lungs[13-15], and the underexplored nature of ECs at single-cell resolution in both diseases, we focused primarily on the EC cohort in our dataset (n = 38,794 nuclei across all three conditions). Using previously published vascular bed marker genes and annotations[22,23,35], 14 transcriptionally distinct EC subclusters could be identified (Figure 2A,B; Figure S1B,C; Table S2). To enable accurate comparisons to other lung single-cell studies, we based our chosen EC subtype nomenclature on a comprehensive integrated single-cell atlas of human lung ECs[23] as much as possible. Specifically, we uncovered: two clusters of arterial ECs (1-2; *GJA5, ARL15, DKK2*), of which artery 2 distinguished itself by increased expression of *IGFBP3* and *CXCL12*; capillary arterial ECs (3), expressing both arterial (*GJA5*) and capillary marker genes (*FCN3*) (representing arteriolar ECs); aerocytes (4; *CA4, ACE, EDNRB*); two clusters of general capillary ECs (5-6; *NOSTRIN, FCN3, BTNL9*), of which cluster 6 additionally expressed inflammatory marker genes (*CX3CL1, ICAM1*); capillary venous ECs (7; *FCN3*, *ACKR1, SELP*) (representing venular ECs) and two clusters of pulmonary venous ECs (8-9; *ACKR1*, *SELP*), of which cluster 9 specifically showed elevated expression of *CPE, PTGIS* and *NRG1*; large vessel ECs (10), expressing both arterial and venous marker genes (*BMX, SELP, EDN1*); the recently described *COL15A1*$^{+}$ peri-bronchial[22] or systemic venous[23] ECs (11; *COL15A1*, *SPRY1, ZNF385D, POSTN*), as well as a *COL15A1*$^{+}$ capillary EC population that we coined 'systemic capillary' ECs (12; *COL15A1, INSR,*

ACCEPTED MANUSCRIPT

ZNF385D) (see below for details); proliferating ECs (13; *MKI67*) and lymphatic ECs (14; *PROX1, MMRN1* (Figure 2A,B)).

We next explored differences in abundance of certain EC subtypes across control, COVID-19 and IPF samples, to investigate whether a differential abundance of certain EC subtypes can be associated with any of these conditions. As a population, ECs were similarly abundant in control, COVID-19 and IPF lungs (Figure 1C,D), but at the subcluster level, we observed an underrepresentation of general capillaries, while systemic venous and capillary EC populations were expanded in both COVID-19 and IPF lungs (Figure 2C,D).

ECs IN LETHAL COVID-19: TRANSCRIPTOME SIGNATURES OF INCREASED STRESS, ALTERED IMMUNE SIGNALING AND PERTURBED BARRIER INTEGRITY

To characterize the global gene expression signatures of the vascular compartment across conditions, we performed differential gene expression analysis (DGEA) and gene set enrichment analysis (GSEA) of all (pooled) COVID-19 or IPF *versus* control ECs (Table S3). These analyses revealed, among others, an enrichment for genes involved in antigen presentation, hypoxia signaling and extracellular matrix (ECM) interactions in COVID-19, while several gene sets related to immune system regulation, inflammation and cell-cell adhesion were negatively enriched (Figure 3A,B). To explore whether the enrichment/depletion of these gene sets was selective to a specific EC subtype, we analyzed the expression of representative genes belonging to these enriched pathways across the major identified EC subtypes (see Supplementary Methods for details on pooling of the different subclusters). We observed that genes encoding heat shock proteins (*HSP90AA1, HSPA1A*) involved in cellular stress were particularly enriched in COVID-19 pulmonary microvascular ECs (Figure 3C), presumably evoked by the harsh microenvironmental conditions in these lungs and the reported endothelialitis[37]. Genes involved in ECM production/remodeling and associated matrix/receptor signaling (*TIMP1, FBN1, MMP16, COL15A1*) were enriched in both COVID-19 and IPF ECs (Figure 3C). This enrichment was observed in arterial and systemic ECs, but was particularly prominent in venous ECs (Figure 3C), and

ACCEPTED MANUSCRIPT

suggests a potential involvement of the vasculature in creating a pro-fibrotic environment in both conditions.

ECs in COVID-19 lungs (and similarly in IPF lungs) furthermore showed decreased expression of certain genes and gene sets involved in immunity/inflammation (chemokines/cytokines, TNF and JAK/STAT signaling), possibly contributing to dampening of the immune response (Figure 3B,C). For instance, transcript levels of immunostimulatory genes including *ICAM1* (leukocyte recruitment/adhesion, and a known marker of EC activation) and *IRF1* (proinflammatory EC activation) were downregulated in both COVID-19 and IPF, as observed in tumor ECs[35,38], across the majority of EC subtypes (Figure 3C). Conversely, levels of *IDO1*, which positively correlates with SARS-CoV-2 viral load in COVID-19 autopsy samples[39], were upregulated in COVID-19 and IPF (arterial/microvascular) ECs (Figure 3C). An increased abundance of $IDO1^+$ ECs ($CD31^+$) was also observed by immunostaining of lung sections in COVID-19 (Figure S1D). While *in vitro* studies suggested immunosuppressive roles of endothelial IDO1, the roles of IDO1 in ECs in the *in vivo* setting are yet to be determined and may be context-dependent. Overall, the immune gene signature in lethal COVID-19 (and IPF) seemed to be complex. For instance, in general capillary ECs, which are considered semi-professional antigen presenting cells[40] and reduced in numbers as a population in COVID-19 (Figure 2C,D), levels of genes involved in antigen processing and presentation were upregulated in COVID-19 (Figure 3C), possibly in an attempt to mount a compensatory immune response. Altogether, ECs in COVID-19 and IPF exhibit an immunosuppressive transcriptome signature, though the relevance of other immunostimulatory gene signatures requires further study.

Consistent with the reported vascular activation and leakage in COVID-19 lungs[37], gene sets involved in cell-cell adhesion were decreased in COVID-19 ECs (Figure 3B,C). For instance, expression of *CDH5,* important for endothelial junction stability, as well as of other genes involved in EC barrier maintenance and vessel wall integrity (*ITGB1*, *RAP1B, CDC42, OCLN, VCL)*[41-43] or vascular quiescence and homeostasis (*S1PR1*) was generally decreased in COVID-19 EC subtypes, most strikingly in aerocytes (Figure 3C). Despite reports of vascular damage in IPF[44], such transcriptome changes were

ACCEPTED MANUSCRIPT

not clearly detected in IPF lung ECs (Figure 3C), raising the question whether impaired EC barrier integrity is a trait more selective to lethal COVID-19. Notably, transcripts of *ANGPT1* (known to tighten the vessel wall and to lower vascular permeability)[45] were reduced only in COVID-19 ECs (mainly in aerocytes), while levels of *ANGPT2,* a context-dependent regulator of vascular leakage, pro-inflammatory signal and predictive biomarker of intensive care unit admission of COVID-19 patients[46], were upregulated (mainly in systemic and lymphatic ECs) in both diseases (Figure 3C).

Gene sets involved in regulating hemostasis, a process derailed in COVID-19 and modulated by ECs[47], were generally not significantly altered across conditions in our dataset (Table S3). In line with this, key genes involved in these processes showed a mixed expression pattern in COVID-19 and IPF ECs, with the expression of the pro-coagulation gene *F8* predominantly being decreased in IPF only, whereas certain anti-coagulation genes (*PROCR, THBD*) were more dominantly decreased in COVID-19 ECs (Figure 3C). Prominent differential expression of *TFPI* (anti-coagulation) and *PLAT* (clot dissolution), on the other hand, could not be clearly detected in COVID-19 and IPF ECs (Figure 3C).

Unbiased hierarchical clustering complemented with multiscale bootstrapping revealed that transcriptomes of microvascular and venous ECs seemed to be most prominently rewired in COVID-19 (Figure 3D), in line with our findings described above. Besides the abovementioned genes and gene sets, gene set variation analysis (GSVA) revealed additional genes and processes, for instance vascular smooth muscle contraction, glycolysis, HIF-1α signaling and others, specifically altered in COVID-19 and/or IPF, warranting further exploration (Figure S2A).

To assess robustness of our findings, we next compared our data to an independent lung snRNA-seq dataset of COVID-19 and control patients[15]. Using unbiased hierarchical clustering, we revealed that most COVID-19-derived EC subtypes from both studies clustered together, and separate from control (or IPF) samples, when analyzing the same set of EC-enriched genes as shown in Figure 3C (Figure S2B). When unbiasedly calculating the set of genes enriched (adjusted p-value ≤ 0.05; log-fold change ≥ 0.25) in the EC-compartment of both studies, we found a set of 127 genes congruently

ACCEPTED MANUSCRIPT

enriched (Figure S2C; Table S3). To evaluate enrichment of these congruent genes in ARDS in a non-COVID-19 context, we generated a bulk RNA-sequencing (RNA-seq) dataset of post-mortem lung tissue from severe COVID-19 and influenza A (H1N1) patients, as well as non-COVID-19 controls (Figure S2D, for clinical information of COVID-19 and influenza patients in this cohort, see[37]). Bulk deconvolution, using our snRNA-seq dataset as a reference, predicted the presence of all major cellular lineages (epithelial, stromal, endothelial and immune cells) in the bulk RNA-seq dataset (Figure S2E). Hierarchical clustering, using the congruent 127-gene signature, revealed that COVID-19 patients clustered separately from control and influenza patients (Figure S2F). Nonetheless, gene expression patterns were largely similar in influenza and COVID-19 patients, but most pronounced in COVID-19 (Figure S2F). Lastly, when analyzing the same set of genes in a bulk RNA-seq dataset of lung tissue from a human ACE2-expressing transgenic (K18-hACE2) mouse model of severe COVID-19[48] (Figure S2G), we observed enriched expression of about half of the EC-enriched end-stage COVID-19 genes, suggesting that the enrichment of at least part of our observed signatures may be COVID-19-associated, and not merely a consequence of general ARDS or cohort-related confounders (e.g. ventilation, treatment regimens).

Altogether, ECs in COVID-19 lungs thus selectively exhibited a signature involved in cellular stress and perturbed barrier maintenance/integrity, and (partially) shared signatures with IPF indicative of increased ECM deposition/remodeling and altered immunomodulation, with on one hand the downregulation of pro-inflammatory genes and adhesion molecules, while on the other hand upregulating multiple genes involved in antigen presentation. These signatures seem, at least in part, specific to and/or more pronounced in late-stage COVID-19.

EC CROSS-TALK WITH OTHER PULMONARY CELL TYPES IN COVID-19 AND IPF

Given the prominent transcriptomic changes in COVID-19 and IPF ECs, we next explored with which other pulmonary cells they were predicted to interact, and which of such interactions might likely explain the altered vascular gene expression landscape. We therefore used all non-vascular cell types

ACCEPTED MANUSCRIPT

in our snRNA-seq data to characterize their cross-talk with ECs in every condition. Given the recently published landscapes of stromal, epithelial and immune cell subtypes in healthy, COVID-19 and IPF lung tissue[13-15,22], we refer to Figures S3-S6, Tables S2-S3 and the Supplementary Methods for a detailed overview of their unsupervised clustering analyses and annotation, as well as their differential abundance in COVID-19 and IPF *versus* control lung tissue. Using CellPhoneDB[49], we characterized the cross-talk between ECs (all subtypes pooled) and other major pulmonary cell types by assessing their predicted receptor-ligand interaction (RLI) landscape. Whereas the full interactome analysis is provided in Table S4, we specifically focused on the interactions between the pulmonary cellular environment and the endothelium (Figure 4A-C; Figure S7A,B). For subtype-specific expression of EC-expressed interaction partners, we refer to Figure S7C. Our analyses revealed several interactions, previously not yet implicated in COVID-19 or IPF pathobiology.

In COVID-19 and IPF, fewer interactions involved in angiogenesis, vascular integrity and homeostasis (EGFR-TGFB1, FGFR1-KL/FGF7, NRP2-SEMA3F, PDGFB-PDGFRA/PDGFRB) were identified within the vascular compartment itself, or between ECs and epithelial or stromal cells (Figure 4A-C). Moreover, among downregulated interactions between the same cell types in COVID-19 was DLL4/JAG1-NOTCH1 signaling (Figure 4A-C). Loss of endothelial NOTCH1 signaling has been associated with perturbed vascular remodeling and a reduction of fenestrae in hepatic sinusoidal ECs, portal hypertension and intussusceptive angiogenesis (IA)[50], an alternative mode of vascularization documented in COVID-19 autopsy samples[37]. Likewise, interactions potentially driving vascular leakage/permeability were also specifically detected in COVID-19, or COVID-19 and IPF. For instance, Ephrin receptor signaling in ECs (EPHA4; predominantly expressed in arterial and systemic ECs), induced by Ephrins (EFNA1, EFNA5) in epithelial and stromal cells (Figure 4B,C; Figure S7C), which may increase EC permeability and vessel leakage[51], was detected in COVID-19 and IPF samples, but not in control lungs. Furthermore, signaling of anti-angiogenic SEMA3A (predicted to be secreted by the endothelium) through its receptors (NRP1, Plexins) on ECs, stromal or epithelial cells, was selectively

ACCEPTED MANUSCRIPT

predicted to occur in COVID-19 (Figure 4A-C), and has been implicated in increasing vascular permeability[52].

On the other hand, certain gene expression signatures suggested possible compensatorily induced repair mechanisms. Indeed, various other interactions uniquely predicted in COVID-19 or in both COVID-19 and IPF were predominantly involved in maintaining vessel integrity. For instance, IGF1, expressed by stromal cells, was predicted to signal through IGF1R on ECs in COVID-19 and IPF (Figure 4C). IGF1 may exert pro-migratory effects on ECs[53], is believed to decrease permeability and may act as a vasodilator[54], all of which might be compensatorily induced to repair the vascular defects in COVID-19 and IPF. Furthermore, COVID-19-selective signaling of HGF (secreted by stromal cells) through the MET receptor on ECs (Figure 4C) may inhibit hypoxia-induced EC apoptosis[55], and is important for EC motility, proliferation and angiogenesis[56].

In line with our abovementioned observations of reduced EC-specific expression of genes involved in immunity/inflammation in COVID-19, among interactions predicted between ECs and immune cells, we observed a selective reduction in cross-talk involved in leukocyte adhesion, recruitment and trans-endothelial migration (JAM2/JAM3 or ICAM1 on ECs with integrin complexes on immune cells) and T cell activation (CD2-CD58 and CD46-JAG1 axes)[57,58] (Figure S7A,B). Interactions involved in myeloid cell recruitment and/or apoptosis (NRP1 on myeloid cells, SEMA3A on (aerocyte and lymphatic) ECs)[59,60] were specifically enriched in COVID-19 lungs (Figure S7A,C). A decrease in signaling involved in pathogen clearance (ANXA1-FPR1/FPR3) was also specifically observed in COVID-19 (Figure S7A). Furthermore, while increased signaling through the GAS6-MERTK/AXL axis (also implicated in clearing of pathogens) was selectively observed in IPF lungs, this interaction was not detected in COVID-19 (Figure S7A), highlighting potential differences between COVID-19 and IPF lung pathology from an immunoregulatory standpoint.

In agreement, we observed a few additional notable differences between COVID-19 EC interactomes and those present in IPF explant lungs. For instance, the interaction of EC-secreted BMP6 (known to exert pro-fibrogenic effects[61]) with BMP receptors on almost all non-EC cell types,

ACCEPTED MANUSCRIPT

and VEGFB (described to contribute to hypoxia-induced vascular remodeling and hypertension in the lung[62]) secretion by epithelial cells, predicted to signal through FLT1/NRP1 on ECs, were both uniquely identified in IPF (Figure 4B,C and Figure S7A,B). Moreover, increased secretion of IL15 by ECs was predicted to signal through IL15RA on stromal cells specifically in the context of COVID-19 (Figure 4C). The expression of IL15 was predominantly present in systemic ECs (Figure S7C), whereas IL15RA was mainly detected in fibroblast subclusters of the stromal cell compartment (Table S2), and complementary NicheNet analysis (Figure S8A), to explore the putative downstream effects of systemic EC-mediated IL15 signaling in COVID-19 fibroblasts, revealed that the glycolytic genes *PKM* and *PGK1* were among downstream target genes regulated by IL15 (Figure S8B). Glycolysis is known to be important for ECM production and the fibrogenic phenotype of fibroblasts[63], and indeed, compared to control or IPF, several members of the glycolysis pathway were upregulated specifically in COVID-19 stromal cells (Figure S8C). These findings may suggest that, despite (partial) commonalities regarding EC-interactomes involved in impaired barrier integrity in lethal COVID-19 and IPF, different drivers of the fibrogenic response and vascular remodeling may underlie both conditions.

INCREASED ABUNDANCE OF THE SYSTEMIC VASCULATURE IN LETHAL COVID-19 AND IPF

As mentioned above, we observed a selective expansion of the systemic (venous and capillary) vasculature in both COVID-19 and IPF lungs, while general capillaries significantly decreased in abundance in both conditions (Figure 2C,D). This observed shift on one hand likely reflects damage of the pulmonary circulation, yet on the other hand may suggest a possible compensatory expansion of the systemic circulation to secure sufficient blood supply, as seen in IPF and other pulmonary diseases[22]. Immunostainings for COL15A1 (used as a canonical marker for peri-bronchial/systemic-venous ECs[22,23]) and CD105 confirmed the bronchial localization of systemic-venous/peri-bronchial ECs in healthy lungs, opposed to a predominant presence in fibrotic regions in COVID-19 lungs (Figure

ACCEPTED MANUSCRIPT

5A), verifying our snRNA-seq findings, and in line with previous observations (see introduction) in IPF lungs[22].

Notably, and unlike previously reported work[22,23], we not only identified a subpopulation of systemic-venous ECs in our dataset, but also a second population of ECs expressing reported markers of the systemic vasculature (*ZNF385D, SPRY1, COL15A1, EBF1*)[22,23], but lacking clear expression of venous marker genes (*ACKR1, HDAC9, SELP*) (Figure 5B). Instead, these ECs more strongly resemble microvascular ECs, based on their expression of markers commonly detected in general capillary ECs (*KDR, RGCC, BTNL9*)[23,35] (Figure 5B). We hypothesized that the discrepancy between our findings and other studies, in which such a microvascular systemic EC subtype was not identified as a transcriptomically separate cluster, is likely due to the substantially higher number of ECs captured in our dataset, allowing us to chart vascular heterogeneity to a larger extent. To explore this further, we extracted single systemic ECs from external, publicly available datasets of either COVID-19[15] or IPF lungs[22,64], and used SingleR[65] to annotate these cells using our systemic EC subclusters as a reference. Indeed, systemic ECs in all three datasets could be separated into venous and microvascular subsets (Figure 5C). This analysis verified the presence of a transcriptomically distinct subcluster of systemic-capillary ECs, thereby adding a thus far overlooked, but additional layer of transcriptional heterogeneity within the pulmonary systemic vascular population. Notably, immunostainings confirmed the presence of both systemic-venous ECs ($COL15A1^+CD105^+$ in direct proximity of αSMA^+ smooth muscle cells) and systemic capillary ECs ($COL15A1^+CD105^+$, distant from αSMA^+ smooth muscle cells) in COVID-19 (and healthy) lungs (Figure S9).

Considering that cellular subtypes, which are congruently altered across different conditions, may represent interesting therapeutic targets, the common enrichment of the systemic vasculature in both COVID-19 and IPF lungs may open interesting avenues for further translational investigation. We therefore performed DGEA, comparing pooled COVID-19 or IPF systemic venous and capillary EC subclusters (jointly referred to as 'systemic ECs') to their control counterparts (using only our in-house generated dataset), to explore robust systemic EC marker genes enriched in both conditions. This

ACCEPTED MANUSCRIPT

analysis revealed a set of 107 common genes, of which several are involved in ECM production/remodeling and associated matrix/receptor signaling (*TIMP2, FBN1, FN1, MMP16, COL15A1, ITGB4, LAMA3, A2M, JAM2*) and cellular migration (*INSR, TGFBR2, MET, CDH13*) (Figure 5D; Table S5), suggesting that systemic ECs in lethal COVID-19 and IPF may be endowed with increased migratory and fibrogenic properties.

To more comprehensively establish a signature of systemic EC marker genes congruently enriched in IPF and COVID-19 across different patient cohorts, we again took advantage of the abovementioned publicly available COVID-19[15] and IPF lung[22,64] datasets to assess similarity of (systemic) ECs across all studies. First, we calculated the top-50 most highly ranking marker genes of all EC subtypes (pooled, see Methods), and used pairwise Jaccard similarity coefficients to reveal that the transcriptomes of EC subtypes (including systemic ECs) are highly conserved across studies (and thus conditions) (Figure 5E). Furthermore, a meta-analysis of marker genes specific to systemic ECs in each dataset revealed a list of 30 congruent genes, significantly enriched in systemic ECs, in all studies in health and disease (Figure 5F,G; Table S5). Within this signature, obtained from independent patient cohorts, experimental setups (single-cell *versus* single-nucleus RNA-seq) and conditions (COVID-19 or IPF), *EPS8*, *ANKRD28, BACE2* and *MCTP1* were also robustly enriched in COVID-19 and IPF systemic ECs (compared to their control counterparts) across studies (Figure 5H). The function of these genes in COVID-19 and IPF, or ECs in general, however remains elusive to date.

Together, ECs in lethal COVID-19 are dominantly enriched for a population of systemic ECs, with high transcriptional resemblance to their counterparts in IPF, suggesting, besides the vast differences in the cause and progression of COVID-19 and IPF, a common EC subtype may contribute to vascular remodeling observed in both conditions.

DISCUSSION

We conducted this pulmonary single-nucleus analysis to identify EC phenotypes exhibiting transcriptome signature changes that might suggest a possible contribution to the vascular problems

ACCEPTED MANUSCRIPT

faced by lethal COVID-19 patients. Moreover, we aimed to compare EC transcriptomes between COVID-19 and IPF lungs, to pinpoint key similarities and differences between two conditions characterized by progressive fibrotic lung disease. Our study, in which we profiled >35,000 ECs extracted from post-mortem biopsies of COVID-19 and control lungs, as well as IPF explant lungs, resulted in multiple novel insights.

First, we observed a gene expression signature suggestive of vascular leakage, decreased barrier integrity and possible dampened immunity in the vascular compartment of COVID-19 and (to some extent) IPF lungs (Figure 6). Of note, while changes in RNA abundance may not always be informative for inference of final protein activity, the functional roles for some of our identified barrier-associated genes may be context-dependent, the downregulation of only one tight junction protein may be compensated by others, and vascular barrier regulation by these junctional molecules also relies at levels beyond mRNA transcription, our results are based on the downregulation of a group of genes involved in these processes, not a single gene. Alongside the plethora of indications of vascular leakage in other studies of COVID-19 lung disease[17,37,66], our results are thus in line with the concept of vascular leakage as a key hallmark of end-stage COVID-19. Moreover, our data highlight prominent transcriptome rewiring of barrier-related genes in the aerocyte (important for gas exchange, and part of the blood-air barrier)[67] and general capillary compartments of the pulmonary vasculature, both of which are shown to localize to the alveolar wall of the lung[23], possibly in line with the extensive alveolar damage reported in severe COVID-19 patients[68].

Our EC-centered interactome analysis, based on predictions requiring further validation, confirmed these observations and further revealed various routes of EC-microenvironmental cross-talk that could potentially drive this dysfunctional state of the vasculature, predominantly driven by decreased EC – non-EC signaling involved in general vascular integrity and homeostasis (Figure 6), together revealing novel insights into and suggesting potential drivers of vascular derailment in fibrotic lung conditions. In addition, EC activation is commonly reported as a key characteristic in acute COVID-19, yet our results (e.g. decreased expression of *ICAM1, IRF1)* may reflect a potential

ACCEPTED MANUSCRIPT

dampening of EC-mediated immune responses in lethal COVID-19. While in tumour ECs, downregulation of immunostimulatory genes is considered an immune escape mechanism of the tumour, in chronic disease conditions like COVID-19 and IPF, it may potentially present a compensatory mechanism to thwart the uncontrollable inflammation in the tissue. On the other hand, the immune gene signature of ECs in lethal COVID-19 (and IPF) seemed to be complex, as we also found evidence for reduced levels of *CD274* (encoding PD-L1), an immune checkpoint inhibitor[69], in both COVID-19 and IPF, while levels of genes involved in antigen processing and presentation were upregulated primarily in COVID-19. Whereas certain hallmarks of EC activation (e.g. loss of vascular integrity, upregulation of HLA genes) are thus apparent in the transcriptome signature of lethal COVID-19 ECs, other hallmarks (upregulation of leukocyte adhesion molecules) are absent, possibly highlighting important vascular differences between early (acute) and lethal disease stages in COVID-19 lungs, warranting further investigation into the (translational) relevance of our identified gene signatures.

Second, while single-cell resolution studies of post-mortem lung tissue in other types of ARDS are currently lacking, our comparative analyses suggest that the transcriptomic changes observed in COVID-19 (ECs) can in part also be found in lungs of SARS-CoV-2 infected mice, suggesting that, at least to a substantial extent, these changes are independent of potential confounding factors inherently present in patient cohorts (e.g. underlying health conditions, treatment regimen, post-mortem ischemia, etc.). Moreover, although bulk RNA-seq informs on general transcriptional signatures and thus cannot particularly inform on EC-selective transcriptome changes, we observed similar expression patterns of a COVID-19 enriched, EC-specific gene expression signature in bulk RNA-seq data of COVID-19 and influenza-associated ARDS lung samples. However, changes were most pronounced in COVID-19.

Third, whereas the overall abundance of the COVID-19 and IPF pulmonary vascular compartment was unchanged in comparison to control lungs, we observed a significant reduction of general capillaries in both conditions. We did not specifically observe an enrichment in (regenerative)

ACCEPTED MANUSCRIPT

proliferating ECs as reported in the resolution phase of influenza infection in mice[70]. Differences in species and disease type/severity/staging may have caused this discrepancy between the two studies. The systemic EC population, within which we identified a thus far overlooked microvascular population, was significantly enriched in both COVID-19 and IPF lungs, compared to the control setting. In line with reports on inflammatory lung disease[71], these findings suggest that the systemic EC phenotype may possibly be triggered to induce repair of the damaged pulmonary circulation in COVID-19 (Figure 6).

However, the transcriptome signature of systemic ECs presented with a notable enrichment for genes involved in ECM remodeling/organization and migration in both COVID-19 and IPF. Interactome analysis furthermore suggested a selective interaction between IL15, predicted to be secreted predominantly by systemic ECs, and IL15RA expressed on stromal cells. By possibly stimulating glycolysis, our data may suggest that systemic ECs, besides their potential intrinsic pro-fibrotic properties, could also act as a driver of the fibrogenic response of stromal cells. Altogether, these findings may indicate a possible contribution of the systemic vasculature to progressive pulmonary fibrosis, raising the question whether targeting the systemic vasculature may represent a plausible anti-fibrotic strategy. However, considering their likely contribution to tissue repair, an optimal targeting strategy could entail specific inhibition of their pro-fibrotic or potential pathological properties, instead of a complete impediment of the systemic vasculature. In that light, our integrated meta-analysis revealed a set of 30 genes robustly expressed by systemic ECs across different COVID-19 and IPF studies, patient cohorts and sequencing strategies, with 4 genes robustly upregulated in the disease context, and may thus represent a good starting point for further study into the functional and/or pathological role of these candidates in the systemic vasculature. Whether systemic venous and capillary ECs might, despite their partially overlapping transcriptomes, exhibit distinct functions during either the fibrotic response or vascular repair remains to be elucidated. Notably, the fibrotic response also involves stromal cell types (in which ECM remodeling-related genes/processes were also found upregulated in COVID-19 (Figure S5G,H)), which have to be considered in this context as

ACCEPTED MANUSCRIPT

well.

We acknowledge that our findings are limited by the patient cohort size, COVID-19-associated confounders (e.g. prolonged mechanical ventilation, therapeutic regimens) and require further, functional validation. Furthermore, while in lethal/end-stage COVID-19 patients the virus is considered to no longer actively replicate[72], we did not determine active SARS-CoV-2 infection at the time of death in our patient cohort. We also cannot exclude the possibility that treatment with corticosteroids might have affected (in part) the observed transcriptomic landscape in severe COVID-19 tissues, including the decreased expression of immunoregulatory genes. Nonetheless, the analyzed samples are comparable to previous COVID-19 lung/tissue atlases[14,15], and representative of patients who received the standard-of-care treatments given in the respective clinical setting. While the therapeutic implications of our findings remain elusive, our study has nevertheless contributed to unraveling the heterogeneous composition and potential functions of the vasculature in COVID-19 and IPF lungs, and provides a rich resource for exploration of both vascular and non-vascular cell types in the context of progressive pulmonary fibrosis in these two lethal conditions. In addition, since pulmonary fibrosis is often a long-term consequence of severe COVID-19, we speculate that the abundant presence of systemic ECs may not only pose problems for acute COVID-19 patients, but also for COVID-19 survivors. This is particularly relevant in the context of long COVID, a condition in which the vasculature may play an important role as well[73]. Lastly, given the current scarcity of model systems that accurately reflect severe/lethal COVID-19, our results shed important novel light into the gene expression landscape of the vasculature in this affliction, and may open up future opportunities regarding screening, monitoring and therapeutic management of (long) COVID patients.

FUNDING

This work was supported by the 'Fonds Wetenschappelijk Onderzoek' (FWO; L.D.R., L.M.B, A-C.K.T., K.R., M.B., J.A. and P.V.M.); Leuven University (L.A.T.); a Marie Skłodowska-Curie-individual fellowship

ACCEPTED MANUSCRIPT

(L.M.B., J.A. and S.J.D.), Strategisch Basisonderzoek FWO (SB-FWO; V.G.); Broere Charitable Foundation (D.V.R); the clinical research and education council of the University Hospitals Leuven (J.G.); Stichting tegen Kanker (Mandate for basic & clinical oncology research; E.W.); Covid-19-Fund KU Leuven/UZ Leuven and FWO (G0G4820N; J.N.); FWO Fundamental Clinical Mandate (1833317N; J.W.); European Research Council Consolidator Grant (XHale) (771883; D.J.); Methusalem funding, FWO, ERC Proof of Concept (ERC-713758), and Advanced ERC Research Grant (EU-ERC743074; P.C.). The computational resources used in this work were partly provided by the Flemish Supercomputer Center (VSC), funded by the Hercules Foundation and the Flemish Government, Department of Economy, Science and Innovation (EWI).

AUTHOR CONTRIBUTION STATEMENT

L.D.R. and L.M.B. designed and analyzed experiments. B.B. and G.P. performed QC and mapping of transcriptomics data. L.A.T., S.J., L.L, T.V.B., S.J.D., E.M, M.B., L. Sokol, A-C.K.T, K.R., R.B., V.G. and J.A. performed experiments and/or provided (experimental) support. S.Vinckier performed immunohistochemistry. S.F., S.Verleden, A.K.S., S.L., A.D., J.G., P.V.M., J.D.H., T.M., M.K., D.J., V.G., W.W., D.V.R., W.J., L.J.C., B.W., M.L., J.V.D., A.T., E.W. and J.W. contributed to the collection of clinical specimens. L.D.R., L.M.B. and P.C. wrote the manuscript. G.E., M.D. and L.Schoonjans supervised the study. B.T., M.M., J.N. and D.L. provided insights and/or resources. L.Schoonjans and P.C. contributed to project administration and funding acquisition. P.C. conceptualized the study. All authors approved the manuscript.

ACKNOWLEDGMENTS

The authors gratefully acknowledge Ann Manderveld, An Carton, Thomas van Brussel, Rogier Schepers, Naima Dai, Christophe Hermans, Toine Mercier and Koen De Winne for technical assistance.

ACCEPTED MANUSCRIPT

CONFLICT OF INTEREST

The authors declare no conflict of interest.

DATA AVAILABILITY

All raw and processed sequencing data generated during this study are available at GEO, under accession code GSE159585. Raw sequencing counts and accompanying annotations can moreover be found at https://carmelietlab.sites.vib.be/Data access. This study did not generate any new code.

ACCEPTED MANUSCRIPT

REFERENCES

1 Gibson, P. G., Qin, L. & Puah, S. H. COVID-19 acute respiratory distress syndrome (ARDS): clinical features and differences from typical pre-COVID-19 ARDS. *The Medical journal of Australia* **213**, 54-56.e51, doi:10.5694/mja2.50674 (2020).

2 Tregoning, J. S., Flight, K. E., Higham, S. L., Wang, Z. & Pierce, B. F. Progress of the COVID-19 vaccine effort: viruses, vaccines and variants versus efficacy, effectiveness and escape. *Nature Reviews Immunology* **21**, 626-636, doi:10.1038/s41577-021-00592-1 (2021).

3 Shang, L., Lye, D. C. & Cao, B. Contemporary narrative review of treatment options for COVID-19. *Respirology* **26**, 745-767, doi:https://doi.org/10.1111/resp.14106 (2021).

4 Liao, M., Liu, Y., Yuan, J., Wen, Y., Xu, G., Zhao, J., Cheng, L., Li, J., Wang, X., Wang, F., Liu, L., Amit, I., Zhang, S. & Zhang, Z. Single-cell landscape of bronchoalveolar immune cells in patients with COVID-19. *Nat Med* **26**, 842-844, doi:10.1038/s41591-020-0901-9 (2020).

5 Wilk, A. J., Rustagi, A., Zhao, N. Q., Roque, J., Martinez-Colon, G. J., McKechnie, J. L., Ivison, G. T., Ranganath, T., Vergara, R., Hollis, T., Simpson, L. J., Grant, P., Subramanian, A., Rogers, A. J. & Blish, C. A. A single-cell atlas of the peripheral immune response in patients with severe COVID-19. *Nat Med*, doi:10.1038/s41591-020-0944-y (2020).

6 Wauters, E., Van Mol, P., Garg, A. D., Jansen, S., Van Herck, Y., Vanderbeke, L., Bassez, A., Boeckx, B., Malengier-Devlies, B., Timmerman, A., Van Brussel, T., Van Buyten, T., Schepers, R., Heylen, E., Dauwe, D., Dooms, C., Gunst, J., Hermans, G., Meersseman, P., Testelmans, D., Yserbyt, J., Tejpar, S., De Wever, W., Matthys, P., Bosisio, M., Casaer, M., De Smet, F., De Munter, P., Humblet-Baron, S., Liston, A., Lorent, N., Martinod, K., Proost, P., Raes, J., Thevissen, K., Vos, R., Weynand, B., Wouters, C., Neyts, J., Wauters, J., Qian, J., Lambrechts, D. & collaborators, C. Discriminating mild from critical COVID-19 by innate and adaptive immune single-cell profiling of bronchoalveolar lavages. *Cell Research*, doi:10.1038/s41422-020-00455-9 (2021).

7 Zhang, J.-Y., Wang, X.-M., Xing, X., Xu, Z., Zhang, C., Song, J.-W., Fan, X., Xia, P., Fu, J.-L., Wang, S.-Y., Xu, R.-N., Dai, X.-P., Shi, L., Huang, L., Jiang, T.-J., Shi, M., Zhang, Y., Zumla, A., Maeurer, M., Bai, F. & Wang, F.-S. Single-cell landscape of immunological responses in patients with COVID-19. *Nature Immunology* **21**, 1107-1118, doi:10.1038/s41590-020-0762-x (2020).

8 Mathew, D., Giles, J. R., Baxter, A. E., Oldridge, D. A., Greenplate, A. R., Wu, J. E., Alanio, C., Kuri-Cervantes, L., Pampena, M. B., D'Andrea, K., Manne, S., Chen, Z., Huang, Y. J., Reilly, J. P., Weisman, A. R., Ittner, C. A. G., Kuthuru, O., Dougherty, J., Nzingha, K., Han, N., Kim, J., Pattekar, A., Goodwin, E. C., Anderson, E. M., Weirick, M. E., Gouma, S., Arevalo, C. P., Bolton, M. J., Chen, F., Lacey, S. F., Ramage, H., Cherry, S., Hensley, S. E., Apostolidis, S. A., Huang, A. C., Vella, L. A., Betts, M. R., Meyer, N. J. & Wherry, E. J. Deep immune profiling of COVID-19 patients reveals distinct immunotypes with therapeutic implications. *Science* **369**, eabc8511, doi:10.1126/science.abc8511 (2020).

9 Wen, W., Su, W., Tang, H., Le, W., Zhang, X., Zheng, Y., Liu, X., Xie, L., Li, J., Ye, J., Dong, L., Cui, X., Miao, Y., Wang, D., Dong, J., Xiao, C., Chen, W. & Wang, H. Immune cell profiling of COVID-19 patients in the recovery stageby single-cell sequencing. *Cell Discovery* **6**, 31, doi:10.1038/s41421-020-0168-9 (2020).

10 Wang, W., Su, B., Pang, L., Qiao, L., Feng, Y., Ouyang, Y., Guo, X., Shi, H., Wei, F., Su, X., Yin, J., Jin, R. & Chen, D. High-dimensional immune profiling by mass cytometry revealed

ACCEPTED MANUSCRIPT

immunosuppression and dysfunction of immunity in COVID-19 patients. *Cellular & molecular immunology* **17**, 650-652, doi:10.1038/s41423-020-0447-2 (2020).

11 Huang, L., Shi, Y., Gong, B., Jiang, L., Liu, X., Yang, J., Tang, J., You, C., Jiang, Q., Long, B., Zeng, T., Luo, M., Zeng, F., Zeng, F., Wang, S., Yang, X. & Yang, Z. Blood single cell immune profiling reveals the interferon-MAPK pathway mediated adaptive immune response for COVID-19. *medRxiv*, 2020.2003.2015.20033472, doi:10.1101/2020.03.15.20033472 (2020).

12 Ren, X., et al. COVID-19 immune features revealed by a large-scale single cell transcriptome atlas. *Cell*, doi:https://doi.org/10.1016/j.cell.2021.01.053 (2021).

13 Bharat, A., Querrey, M., Markov, N. S., Kim, S., Kurihara, C., Garza-Castillon, R., Manerikar, A., Shilatifard, A., Tomic, R., Politanska, Y., Abdala-Valencia, H., Yeldandi, A. V., Lomasney, J. W., Misharin, A. V. & Budinger, G. R. S. Lung transplantation for patients with severe COVID-19. *Science Translational Medicine* **12**, eabe4282, doi:10.1126/scitranslmed.abe4282 (2020).

14 Delorey, T. M., Ziegler, C. G. K., Heimberg, G., Normand, R., Yang, Y., Segerstolpe, Å., Abbondanza, D., Fleming, S. J., Subramanian, A., Montoro, D. T., Jagadeesh, K. A., Dey, K. K., Sen, P., Slyper, M., Pita-Juárez, Y. H., Phillips, D., Biermann, J., Bloom-Ackermann, Z., Barkas, N., Ganna, A., Gomez, J., Melms, J. C., Katsyv, I., Normandin, E., Naderi, P., Popov, Y. V., Raju, S. S., Niezen, S., Tsai, L. T. Y., Siddle, K. J., Sud, M., Tran, V. M., Vellarikkal, S. K., Wang, Y., Amir-Zilberstein, L., Atri, D. S., Beechem, J., Brook, O. R., Chen, J., Divakar, P., Dorceus, P., Engreitz, J. M., Essene, A., Fitzgerald, D. M., Fropf, R., Gazal, S., Gould, J., Grzyb, J., Harvey, T., Hecht, J., Hether, T., Jané-Valbuena, J., Leney-Greene, M., Ma, H., McCabe, C., McLoughlin, D. E., Miller, E. M., Muus, C., Niemi, M., Padera, R., Pan, L., Pant, D., Pe'er, C., Pfiffner-Borges, J., Pinto, C. J., Plaisted, J., Reeves, J., Ross, M., Rudy, M., Rueckert, E. H., Siciliano, M., Sturm, A., Todres, E., Waghray, A., Warren, S., Zhang, S., Zollinger, D. R., Cosimi, L., Gupta, R. M., Hacohen, N., Hibshoosh, H., Hide, W., Price, A. L., Rajagopal, J., Tata, P. R., Riedel, S., Szabo, G., Tickle, T. L., Ellinor, P. T., Hung, D., Sabeti, P. C., Novak, R., Rogers, R., Ingber, D. E., Jiang, Z. G., Juric, D., Babadi, M., Farhi, S. L., Izar, B., Stone, J. R., Vlachos, I. S., Solomon, I. H., Ashenberg, O., Porter, C. B. M., Li, B., Shalek, A. K., Villani, A.-C., Rozenblatt-Rosen, O. & Regev, A. COVID-19 tissue atlases reveal SARS-CoV-2 pathology and cellular targets. *Nature* **595**, 107-113, doi:10.1038/s41586-021-03570-8 (2021).

15 Melms, J. C., Biermann, J., Huang, H., Wang, Y., Nair, A., Tagore, S., Katsyv, I., Rendeiro, A. F., Amin, A. D., Schapiro, D., Frangieh, C. J., Luoma, A. M., Filliol, A., Fang, Y., Ravichandran, H., Clausi, M. G., Alba, G. A., Rogava, M., Chen, S. W., Ho, P., Montoro, D. T., Kornberg, A. E., Han, A. S., Bakhoum, M. F., Anandasabapathy, N., Suárez-Fariñas, M., Bakhoum, S. F., Bram, Y., Borczuk, A., Guo, X. V., Lefkowitch, J. H., Marboe, C., Lagana, S. M., Del Portillo, A., Zorn, E., Markowitz, G. S., Schwabe, R. F., Schwartz, R. E., Elemento, O., Saqi, A., Hibshoosh, H., Que, J. & Izar, B. A molecular single-cell lung atlas of lethal COVID-19. *Nature* **595**, 114-119, doi:10.1038/s41586-021-03569-1 (2021).

16 Varga, Z., Flammer, A. J., Steiger, P., Haberecker, M., Andermatt, R., Zinkernagel, A. S., Mehra, M. R., Schuepbach, R. A., Ruschitzka, F. & Moch, H. Endothelial cell infection and endotheliitis in COVID-19. *Lancet (London, England)* **395**, 1417-1418, doi:10.1016/S0140-6736(20)30937-5 (2020).

17 Teuwen, L.-A., Geldhof, V., Pasut, A. & Carmeliet, P. COVID-19: the vasculature unleashed. *Nature Reviews Immunology* **20**, 389-391, doi:10.1038/s41577-020-0343-0 (2020).

18 Sarelius, I. H. & Glading, A. J. Control of vascular permeability by adhesion molecules. *Tissue barriers* **3**, e985954-e985954, doi:10.4161/21688370.2014.985954 (2015).

19 Levolger, S., Bokkers, R. P. H., Wille, J., Kropman, R. H. J. & de Vries, J.-P. P. M. Arterial thrombotic complications in COVID-19 patients. *Journal of Vascular Surgery Cases and Innovative Techniques* **6**, 454-459, doi:10.1016/j.jvscit.2020.06.012 (2020).

ACCEPTED MANUSCRIPT

20 Dull Randal, O. & Garcia Joe, G. N. Leukocyte-Induced Microvascular Permeability. *Circulation Research* **90**, 1143-1144, doi:10.1161/01.RES.0000023047.87638.76 (2002).

21 Suresh, K. & Shimoda, L. A. Lung Circulation. *Comprehensive Physiology* **6**, 897-943, doi:10.1002/cphy.c140049 (2016).

22 Adams, T. S., Schupp, J. C., Poli, S., Ayaub, E. A., Neumark, N., Ahangari, F., Chu, S. G., Raby, B. A., DeIuliis, G., Januszyk, M., Duan, Q., Arnett, H. A., Siddiqui, A., Washko, G. R., Homer, R., Yan, X., Rosas, I. O. & Kaminski, N. Single-cell RNA-seq reveals ectopic and aberrant lung-resident cell populations in idiopathic pulmonary fibrosis. *Science Advances* **6**, eaba1983, doi:10.1126/sciadv.aba1983 (2020).

23 Schupp, J. C., Adams, T. S., Cosme Jr, C., Raredon, M. S. B., Yuan, Y., Omote, N., Poli, S., Chioccioli, M., Rose, K.-A., Manning, E. P., Sauler, M., DeIuliis, G., Ahangari, F., Neumark, N., Habermann, A. C., Gutierrez, A. J., Bui, L. T., Lafyatis, R., Pierce, R. W., Meyer, K. B., Nawijn, M. C., Teichmann, S. A., Banovich, N. E., Kropski, J. A., Niklason, L. E., Pe'er, D., Yan, X., Homer, R. J., Rosas, I. O. & Kaminski, N. Integrated Single Cell Atlas of Endothelial Cells of the Human Lung. *Circulation* **0**, doi:10.1161/CIRCULATIONAHA.120.052318 (2021).

24 Wigén, J., Löfdahl, A., Bjermer, L., Elowsson Rendin, L. & Westergren-Thorsson, G. Converging pathways in pulmonary fibrosis and Covid-19 - The fibrotic link to disease severity. *Respiratory Medicine: X* **2**, 100023, doi:https://doi.org/10.1016/j.yrmex.2020.100023 (2020).

25 Lechowicz, K., Drożdżal, S., Machaj, F., Rosik, J., Szostak, B., Zegan-Barańska, M., Biernawska, J., Dabrowski, W., Rotter, I. & Kotfis, K. COVID-19: The Potential Treatment of Pulmonary Fibrosis Associated with SARS-CoV-2 Infection. *Journal of clinical medicine* **9**, 1917, doi:10.3390/jcm9061917 (2020).

26 Barratt, S. & Millar, A. Vascular remodelling in the pathogenesis of idiopathic pulmonary fibrosis. *QJM : monthly journal of the Association of Physicians* **107**, 515-519, doi:10.1093/qjmed/hcu012 (2014).

27 Grillo, F., Barisione, E., Ball, L., Mastracci, L. & Fiocca, R. Lung fibrosis: an undervalued finding in COVID-19 pathological series. *The Lancet Infectious Diseases*, doi:10.1016/S1473-3099(20)30582-X.

28 Vasarmidi, E., Tsitoura, E., Spandidos, D. A., Tzanakis, N. & Antoniou, K. M. Pulmonary fibrosis in the aftermath of the COVID-19 era (Review). *Experimental and therapeutic medicine* **20**, 2557-2560, doi:10.3892/etm.2020.8980 (2020).

29 Ojo, A. S., Balogun, S. A., Williams, O. T. & Ojo, O. S. Pulmonary Fibrosis in COVID-19 Survivors: Predictive Factors and Risk Reduction Strategies. *Pulmonary Medicine* **2020**, 6175964, doi:10.1155/2020/6175964 (2020).

30 Slyper, M., Porter, C. B. M., Ashenberg, O., Waldman, J., Drokhlyansky, E., Wakiro, I., Smillie, C., Smith-Rosario, G., Wu, J., Dionne, D., Vigneau, S., Jané-Valbuena, J., Tickle, T. L., Napolitano, S., Su, M.-J., Patel, A. G., Karlstrom, A., Gritsch, S., Nomura, M., Waghray, A., Gohil, S. H., Tsankov, A. M., Jerby-Arnon, L., Cohen, O., Klughammer, J., Rosen, Y., Gould, J., Nguyen, L., Hofree, M., Tramontozzi, P. J., Li, B., Wu, C. J., Izar, B., Haq, R., Hodi, F. S., Yoon, C. H., Hata, A. N., Baker, S. J., Suvà, M. L., Bueno, R., Stover, E. H., Clay, M. R., Dyer, M. A., Collins, N. B., Matulonis, U. A., Wagle, N., Johnson, B. E., Rotem, A., Rozenblatt-Rosen, O. & Regev, A. A single-cell and single-nucleus RNA-Seq toolbox for fresh and frozen human tumors. *Nature medicine* **26**, 792-802, doi:10.1038/s41591-020-0844-1 (2020).

31 Travaglini, K. J., Nabhan, A. N., Penland, L., Sinha, R., Gillich, A., Sit, R. V., Chang, S., Conley, S. D., Mori, Y., Seita, J., Berry, G. J., Shrager, J. B., Metzger, R. J., Kuo, C. S., Neff, N., Weissman, I. L., Quake, S. R. & Krasnow, M. A. A molecular cell atlas of the human lung from single-cell RNA sequencing. *Nature* **587**, 619-625, doi:10.1038/s41586-020-2922-4 (2020).

ACCEPTED MANUSCRIPT

32 Harris, W. T., Kelly, D. R., Zhou, Y., Wang, D., Macewen, M., Hagood, J. S., Clancy, J. P., Ambalavanan, N. & Sorscher, E. J. Myofibroblast Differentiation and Enhanced Tgf-B Signaling in Cystic Fibrosis Lung Disease. *PLOS ONE* **8**, e70196, doi:10.1371/journal.pone.0070196 (2013).

33 Habermann, A. C., Gutierrez, A. J., Bui, L. T., Yahn, S. L., Winters, N. I., Calvi, C. L., Peter, L., Chung, M.-I., Taylor, C. J., Jetter, C., Raju, L., Roberson, J., Ding, G., Wood, L., Sucre, J. M. S., Richmond, B. W., Serezani, A. P., McDonnell, W. J., Mallal, S. B., Bacchetta, M. J., Loyd, J. E., Shaver, C. M., Ware, L. B., Bremner, R., Walia, R., Blackwell, T. S., Banovich, N. E. & Kropski, J. A. Single-cell RNA sequencing reveals profibrotic roles of distinct epithelial and mesenchymal lineages in pulmonary fibrosis. *Science advances* **6**, eaba1972-eaba1972, doi:10.1126/sciadv.aba1972 (2020).

34 Noble, P. W. & Homer, R. J. Back to the Future. *American Journal of Respiratory Cell and Molecular Biology* **33**, 113-120, doi:10.1165/rcmb.F301 (2005).

35 Goveia, J., Rohlenova, K., Taverna, F., Treps, L., Conradi, L.-C., Pircher, A., Geldhof, V., de Rooij, L. P. M. H., Kalucka, J., Sokol, L., García-Caballero, M., Zheng, Y., Qian, J., Teuwen, L.-A., Khan, S., Boeckx, B., Wauters, E., Decaluwé, H., De Leyn, P., Vansteenkiste, J., Weynand, B., Sagaert, X., Verbeken, E., Wolthuis, A., Topal, B., Everaerts, W., Bohnenberger, H., Emmert, A., Panovska, D., De Smet, F., Staal, F. J. T., McLaughlin, R. J., Impens, F., Lagani, V., Vinckier, S., Mazzone, M., Schoonjans, L., Dewerchin, M., Eelen, G., Karakach, T. K., Yang, H., Wang, J., Bolund, L., Lin, L., Thienpont, B., Li, X., Lambrechts, D., Luo, Y. & Carmeliet, P. An Integrated Gene Expression Landscape Profiling Approach to Identify Lung Tumor Endothelial Cell Heterogeneity and Angiogenic Candidates. *Cancer Cell* **37**, 21-36.e13, doi:https://doi.org/10.1016/j.ccell.2019.12.001 (2020).

36 Andreatta, M., Corria-Osorio, J., Müller, S., Cubas, R., Coukos, G. & Carmona, S. J. Projecting single-cell transcriptomics data onto a reference T cell atlas to interpret immune responses. *bioRxiv*, 2020.2006.2023.166546, doi:10.1101/2020.06.23.166546 (2020).

37 Ackermann, M., Verleden, S. E., Kuehnel, M., Haverich, A., Welte, T., Laenger, F., Vanstapel, A., Werlein, C., Stark, H., Tzankov, A., Li, W. W., Li, V. W., Mentzer, S. J. & Jonigk, D. Pulmonary Vascular Endothelialitis, Thrombosis, and Angiogenesis in Covid-19. *New England Journal of Medicine* **383**, 120-128, doi:10.1056/NEJMoa2015432 (2020).

38 Griffioen, A. W., Damen, C. A., Martinotti, S., Blijham, G. H. & Groenewegen, G. Endothelial Intercellular Adhesion Molecule-1 Expression Is Suppressed in Human Malignancies: The Role of Angiogenic Factors. *Cancer Research* **56**, 1111 (1996).

39 Desai, N., Neyaz, A., Szabolcs, A., Shih, A. R., Chen, J. H., Thapar, V., Nieman, L. T., Solovyov, A., Mehta, A., Lieb, D. J., Kulkarni, A. S., Jaicks, C., Xu, K. H., Raabe, M. J., Pinto, C. J., Juric, D., Chebib, I., Colvin, R. B., Kim, A. Y., Monroe, R., Warren, S. E., Danaher, P., Reeves, J. W., Gong, J., Rueckert, E. H., Greenbaum, B. D., Hacohen, N., Lagana, S. M., Rivera, M. N., Sholl, L. M., Stone, J. R., Ting, D. T. & Deshpande, V. Temporal and spatial heterogeneity of host response to SARS-CoV-2 pulmonary infection. *Nature Communications* **11**, 6319, doi:10.1038/s41467-020-20139-7 (2020).

40 Amersfoort, J., Eelen, G. & Carmeliet, P. Immunomodulation by endothelial cells - partnering up with the immune system? *Nat Rev Immunol*, doi:10.1038/s41577-022-00694-4 (2022).

41 Cerutti, C. & Ridley, A. J. Endothelial cell-cell adhesion and signaling. *Experimental Cell Research* **358**, 31-38, doi:https://doi.org/10.1016/j.yexcr.2017.06.003 (2017).

42 Dorland, Y. L. & Huveneers, S. Cell-cell junctional mechanotransduction in endothelial remodeling. *Cellular and molecular life sciences : CMLS* **74**, 279-292, doi:10.1007/s00018-016-2325-8 (2017).

ACCEPTED MANUSCRIPT

43 Glass, J., Robinson, R., Bloom, J., Churchwell, L., Lee, T. J., Sharma, A. & Sharma, S. RNA-Seq reveals IL-6 trans-signaling mediated regulation of paracellular permeability in human retinal endothelial cells. *Investigative Ophthalmology & Visual Science* **62**, 3122-3122 (2021).

44 Probst, C. K., Montesi, S. B., Medoff, B. D., Shea, B. S. & Knipe, R. S. Vascular Permeability in the Fibrotic Lung. *European Respiratory Journal*, 1900100, doi:10.1183/13993003.00100-2019 (2020).

45 Stoeltzing, O., Ahmad, S. A., Liu, W., McCarty, M. F., Wey, J. S., Parikh, A. A., Fan, F., Reinmuth, N., Kawaguchi, M., Bucana, C. D. & Ellis, L. M. Angiopoietin-1 Inhibits Vascular Permeability, Angiogenesis, and Growth of Hepatic Colon Cancer Tumors. *Cancer Research* **63**, 3370 (2003).

46 Smadja, D. M., Guerin, C. L., Chocron, R., Yatim, N., Boussier, J., Gendron, N., Khider, L., Hadjadj, J., Goudot, G., Debuc, B., Juvin, P., Hauw-Berlemont, C., Augy, J.-L., Peron, N., Messas, E., Planquette, B., Sanchez, O., Charbit, B., Gaussem, P., Duffy, D., Terrier, B., Mirault, T. & Diehl, J.-L. Angiopoietin-2 as a marker of endothelial activation is a good predictor factor for intensive care unit admission of COVID-19 patients. *Angiogenesis* **23**, 611-620, doi:10.1007/s10456-020-09730-0 (2020).

47 Teuwen, L. A., Geldhof, V., Pasut, A. & Carmeliet, P. COVID-19: the vasculature unleashed. *Nat Rev Immunol*, doi:10.1038/s41577-020-0343-0 (2020).

48 Winkler, E. S., Bailey, A. L., Kafai, N. M., Nair, S., McCune, B. T., Yu, J., Fox, J. M., Chen, R. E., Earnest, J. T., Keeler, S. P., Ritter, J. H., Kang, L.-I., Dort, S., Robichaud, A., Head, R., Holtzman, M. J. & Diamond, M. S. SARS-CoV-2 infection of human ACE2-transgenic mice causes severe lung inflammation and impaired function. *Nature Immunology*, doi:10.1038/s41590-020-0778-2 (2020).

49 Efremova, M., Vento-Tormo, M., Teichmann, S. A. & Vento-Tormo, R. CellPhoneDB: inferring cell–cell communication from combined expression of multi-subunit ligand–receptor complexes. *Nature Protocols* **15**, 1484-1506, doi:10.1038/s41596-020-0292-x (2020).

50 Dill, M. T., Rothweiler, S., Djonov, V., Hlushchuk, R., Tornillo, L., Terracciano, L., Meili–Butz, S., Radtke, F., Heim, M. H. & Semela, D. Disruption of Notch1 Induces Vascular Remodeling, Intussusceptive Angiogenesis, and Angiosarcomas in Livers of Mice. *Gastroenterology* **142**, 967-977.e962, doi:10.1053/j.gastro.2011.12.052 (2012).

51 Woodruff, T., Wu, M., Morgan, M., Bain, N., Jeanes, A., Lipman, J., Ting, M., Taylor, S. & Coulthard, M. Epha4-Fc Treatment Reduces Ischemia/Reperfusion-Induced Intestinal Injury by Inhibiting Vascular Permeability. *Shock (Augusta, Ga.)* **45**, 184-191, doi:10.1097/SHK.0000000000000494 (2016).

52 Hou, S. T., Nilchi, L., Li, X., Gangaraju, S., Jiang, S. X., Aylsworth, A., Monette, R. & Slinn, J. Semaphorin3A elevates vascular permeability and contributes to cerebral ischemia-induced brain damage. *Scientific Reports* **5**, 7890, doi:10.1038/srep07890 (2015).

53 Imrie, H., Viswambharan, H., Sukumar, P., Abbas, A., Cubbon, R. M., Yuldasheva, N., Gage, M., Smith, J., Galloway, S., Skromna, A., Rashid, S. T., Futers, T. S., Xuan, S., Gatenby, V. K., Grant, P. J., Channon, K. M., Beech, D. J., Wheatcroft, S. B. & Kearney, M. T. Novel role of the IGF-1 receptor in endothelial function and repair: studies in endothelium-targeted IGF-1 receptor transgenic mice. *Diabetes* **61**, 2359-2368, doi:10.2337/db11-1494 (2012).

54 Higashi, Y., Sukhanov, S., Shai, S.-Y., Danchuk, S., Snarski, P., Li, Z., Hou, X., Hamblin, M. H., Woods, T. C., Wang, M., Wang, D., Yu, H., Korthuis, R. J., Yoshida, T. & Delafontaine, P. Endothelial deficiency of insulin-like growth factor-1 receptor reduces endothelial barrier function and promotes atherosclerosis in Apoe-deficient mice. *American Journal of Physiology-Heart and Circulatory Physiology* **319**, H730-H743, doi:10.1152/ajpheart.00064.2020 (2020).

ACCEPTED MANUSCRIPT

55 Wang, X., Zhou, Y., Kim, H. P., Song, R., Zarnegar, R., Ryter, S. W. & Choi, A. M. K. Hepatocyte Growth Factor Protects against Hypoxia/Reoxygenation-induced Apoptosis in Endothelial Cells *. *Journal of Biological Chemistry* **279**, 5237-5243, doi:10.1074/jbc.M309271200 (2004).

56 Ding, S., Merkulova-Rainon, T., Han, Z. C. & Tobelem, G. HGF receptor up-regulation contributes to the angiogenic phenotype of human endothelial cells and promotes angiogenesis in vitro. *Blood* **101**, 4816-4822, doi:https://doi.org/10.1182/blood-2002-06-1731 (2003).

57 Mestas, J. & Hughes, C. C. W. Endothelial Cell Costimulation of T Cell Activation Through CD58-CD2 Interactions Involves Lipid Raft Aggregation. *The Journal of Immunology* **167**, 4378, doi:10.4049/jimmunol.167.8.4378 (2001).

58 Le Friec, G., Sheppard, D., Whiteman, P., Karsten, C. M., Shamoun, S. A.-T., Laing, A., Bugeon, L., Dallman, M. J., Melchionna, T., Chillakuri, C., Smith, R. A., Drouet, C., Couzi, L., Fremeaux-Bacchi, V., Köhl, J., Waddington, S. N., McDonnell, J. M., Baker, A., Handford, P. A., Lea, S. M. & Kemper, C. The CD46-Jagged1 interaction is critical for human TH1 immunity. *Nature immunology* **13**, 1213-1221, doi:10.1038/ni.2454 (2012).

59 Ji, J.-D., Park-Min, K.-H. & Ivashkiv, L. B. Expression and function of semaphorin 3A and its receptors in human monocyte-derived macrophages. *Human immunology* **70**, 211-217, doi:10.1016/j.humimm.2009.01.026 (2009).

60 Casazza, A., Laoui, D., Wenes, M., Rizzolio, S., Bassani, N., Mambretti, M., Deschoemaeker, S., Van Ginderachter, Jo A., Tamagnone, L. & Mazzone, M. Impeding Macrophage Entry into Hypoxic Tumor Areas by Sema3A/Nrp1 Signaling Blockade Inhibits Angiogenesis and Restores Antitumor Immunity. *Cancer Cell* **24**, 695-709, doi:https://doi.org/10.1016/j.ccr.2013.11.007 (2013).

61 Hong, J. H., Lee, G. T., Lee, J. H., Kwon, S. J., Park, S. H., Kim, S. J. & Kim, I. Y. Effect of bone morphogenetic protein-6 on macrophages. *Immunology* **128**, e442-e450, doi:10.1111/j.1365-2567.2008.02998.x (2009).

62 Wanstall, J. C., Gambino, A., Jeffery, T. K., Cahill, M. M., Bellomo, D., Hayward, N. K. & Kay, G. F. Vascular endothelial growth factor-B-deficient mice show impaired development of hypoxic pulmonary hypertension. *Cardiovascular Research* **55**, 361-368, doi:10.1016/S0008-6363(02)00440-6 (2002).

63 Zhao, X., Psarianos, P., Ghoraie, L. S., Yip, K., Goldstein, D., Gilbert, R., Witterick, I., Pang, H., Hussain, A., Lee, J. H., Williams, J., Bratman, S. V., Ailles, L., Haibe-Kains, B. & Liu, F.-F. Metabolic regulation of dermal fibroblasts contributes to skin extracellular matrix homeostasis and fibrosis. *Nature Metabolism* **1**, 147-157, doi:10.1038/s42255-018-0008-5 (2019).

64 Reyfman, P. A., Walter, J. M., Joshi, N., Anekalla, K. R., McQuattie-Pimentel, A. C., Chiu, S., Fernandez, R., Akbarpour, M., Chen, C.-I., Ren, Z., Verma, R., Abdala-Valencia, H., Nam, K., Chi, M., Han, S., Gonzalez-Gonzalez, F. J., Soberanes, S., Watanabe, S., Williams, K. J. N., Flozak, A. S., Nicholson, T. T., Morgan, V. K., Winter, D. R., Hinchcliff, M., Hrusch, C. L., Guzy, R. D., Bonham, C. A., Sperling, A. I., Bag, R., Hamanaka, R. B., Mutlu, G. M., Yeldandi, A. V., Marshall, S. A., Shilatifard, A., Amaral, L. A. N., Perlman, H., Sznajder, J. I., Argento, A. C., Gillespie, C. T., Dematte, J., Jain, M., Singer, B. D., Ridge, K. M., Lam, A. P., Bharat, A., Bhorade, S. M., Gottardi, C. J., Budinger, G. R. S. & Misharin, A. V. Single-Cell Transcriptomic Analysis of Human Lung Provides Insights into the Pathobiology of Pulmonary Fibrosis. *Am J Respir Crit Care Med* **199**, 1517-1536, doi:10.1164/rccm.201712-2410OC (2019).

65 Aran, D., Looney, A. P., Liu, L., Wu, E., Fong, V., Hsu, A., Chak, S., Naikawadi, R. P., Wolters, P. J., Abate, A. R., Butte, A. J. & Bhattacharya, M. Reference-based analysis of lung single-cell sequencing reveals a transitional profibrotic macrophage. *Nature Immunology* **20**, 163-172, doi:10.1038/s41590-018-0276-y (2019).

ACCEPTED MANUSCRIPT

66 D'Agnillo, F., Walters, K.-A., Xiao, Y., Sheng, Z.-M., Scherler, K., Park, J., Gygli, S., Rosas Luz, A., Sadtler, K., Kalish, H., Blatti Charles, A., Zhu, R., Gatzke, L., Bushell, C., Memoli Matthew, J., O'Day Steven, J., Fischer Trevan, D., Hammond Terese, C., Lee Raymond, C., Cash, J. C., Powers Matthew, E., O'Keefe Grant, E., Butnor Kelly, J., Rapkiewicz Amy, V., Travis William, D., Layne Scott, P., Kash John, C. & Taubenberger Jeffery, K. Lung epithelial and endothelial damage, loss of tissue repair, inhibition of fibrinolysis, and cellular senescence in fatal COVID-19. *Science Translational Medicine* **13**, eabj7790, doi:10.1126/scitranslmed.abj7790.

67 Gillich, A., Zhang, F., Farmer, C. G., Travaglini, K. J., Tan, S. Y., Gu, M., Zhou, B., Feinstein, J. A., Krasnow, M. A. & Metzger, R. J. Capillary cell-type specialization in the alveolus. *Nature* **586**, 785-789, doi:10.1038/s41586-020-2822-7 (2020).

68 Carsana, L., Sonzogni, A., Nasr, A., Rossi, R. S., Pellegrinelli, A., Zerbi, P., Rech, R., Colombo, R., Antinori, S., Corbellino, M., Galli, M., Catena, E., Tosoni, A., Gianatti, A. & Nebuloni, M. Pulmonary post-mortem findings in a series of COVID-19 cases from northern Italy: a two-centre descriptive study. *The Lancet Infectious Diseases* **20**, 1135-1140, doi:10.1016/S1473-3099(20)30434-5 (2020).

69 Sun, C., Mezzadra, R. & Schumacher, T. N. Regulation and Function of the PD-L1 Checkpoint. *Immunity* **48**, 434-452, doi:10.1016/j.immuni.2018.03.014 (2018).

70 Niethamer, T. K., Stabler, C. T., Leach, J. P., Zepp, J. A., Morley, M. P., Babu, A., Zhou, S. & Morrisey, E. E. Defining the role of pulmonary endothelial cell heterogeneity in the response to acute lung injury. *Elife* **9**, doi:10.7554/eLife.53072 (2020).

71 McCullagh, A., Rosenthal, M., Wanner, A., Hurtado, A., Padley, S. & Bush, A. The bronchial circulation—worth a closer look: A review of the relationship between the bronchial vasculature and airway inflammation. *Pediatric Pulmonology* **45**, 1-13, doi:https://doi.org/10.1002/ppul.21135 (2010).

72 Cevik, M., Tate, M., Lloyd, O., Maraolo, A. E., Schafers, J. & Ho, A. SARS-CoV-2, SARS-CoV, and MERS-CoV viral load dynamics, duration of viral shedding, and infectiousness: a systematic review and meta-analysis. *Lancet Microbe* **2**, e13-e22, doi:10.1016/S2666-5247(20)30172-5 (2021).

73 de Rooij, L. P. M. H., Becker, L. M. & Carmeliet, P. A Role for the Vascular Endothelium in Post–Acute COVID-19? *Circulation* **145**, 1503-1505, doi:10.1161/CIRCULATIONAHA.122.059231 (2022).

ACCEPTED MANUSCRIPT

FIGURE LEGENDS

FIGURE 1: PULMONARY CELL TYPES IN COVID-19, IPF AND CONTROL LUNGS

A, UMAP plot of lung cells from 7 deceased COVID-19 patients, 6 IPF patients who required lung transplantation, and 12 SARS-CoV-2 uninfected controls (who died of causes unrelated to lung disease), color-coded by major cellular lineage. **B,** Dot plot heatmap of expression of representative marker genes of major cellular lineages. The size and color intensity of each dot represent respectively the percentage of cells within each cell type expressing the marker gene and the average level of expression of the marker in this cell type. Color scale: red, high expression; blue, low expression. **C,** UMAP plot of lung cells, color-coded for the indicated conditions. **D,** Fractions of major cell types in COVID-19, IPF and control samples. Mean ±SEM, Kruskal-Wallis and Dunn's test for multiple comparisons, *p < 0.05, **p < 0.01. n=7, 6 and 12 for COVID-19, IPF and control, respectively. **E,** Representative images of lung sections from COVID-19 and control subjects, immunostained for the epithelial marker cytokeratin-7 (CK7; brown). Quantifications of the CK7-positive area (% of the total tissue area) are provided to the right of the images. Scale bar: 25 µm. Mean ±SEM, unpaired t-test, two-tailed, ***p < 0.001, n = 5 and 5 for COVID-19 and control, respectively. **F,** Representative images of lung sections from COVID-19 and control subjects, immunostained for the stromal marker alpha smooth muscle actin (αSMA; brown). Scale bar: 25 µm. Quantifications of the αSMA-positive area (% of the total tissue area) are provided to the right of the images. Data are mean ±SEM, unpaired t-test with Welch correction, two-tailed, *p < 0.05, n = 5 and 5 for COVID-19 and control, respectively. **G,** Overview of the 61 different subclusters identified in epithelial, stromal, endothelial and immune lineages (for a description of all subclusters and their marker genes, see Supplementary Methods).

FIGURE 2: VASCULAR SUBCLUSTERS IN COVID-19, IPF AND CONTROL LUNGS

A, UMAP plot of EC transcriptomes, color- and number-coded for the 14 subtypes identified by graph-based clustering. **B,** Dot plot heatmap of the expression of EC subtype-specific marker genes used for subcluster annotation. The size and color intensity of each dot represent respectively the percentage

ACCEPTED MANUSCRIPT

of cells within each cell type expressing the marker gene and the average level of expression of the marker in this cell type. Color scale: red, high expression; blue, low expression. **C,** UMAP plots of ECs, color-coded per condition **D,** Fraction of EC subtypes in COVID-19, IPF and control samples. Data are mean ±SEM, Kruskal-Wallis and Dunn's test for multiple comparisons, n = 7 (COVID-19), 6 (IPF), 12 (controls), *p < 0.05, **p<0.01.

FIGURE 3: TRANSCRIPTOMIC REWIRING OF COVID-19 AND IPF ECS

A, Volcano plot comparing differentially expressed genes in ECs from COVID-19 versus control lungs. Representative genes are indicated; each dot represents a single gene. Red and grey dots indicate up- or downregulated genes with a false discovery rate (*q* value) < 0.05 or > 0.05, respectively. **B,** Gene set enrichment analysis in ECs derived from COVID-19 lungs, compared with those from controls, using KEGG gene sets. Red bar graphs indicate upregulated gene sets, blue bar graphs indicate downregulated gene sets in COVID-19 ECs. **C,** Gene expression heatmap of individual genes included in the KEGG gene sets presented in (B), in the indicated cell types and conditions. Color scale: red, high expression; blue, low expression. EC subtypes were pooled into major artery (EC1-3), aerocyte (EC4), general capillary (cap; EC5-6), vein (EC7-9), systemic (EC11-12) and lymphatic (EC14) subgroups. NES: normalized enrichment score. **D,** Hierarchical clustering analysis of major (pooled) EC subtypes. Grey and blue dashed boxes indicate clusters that were resolved by multiscale bootstrapping (approximately unbiased (AU) p-value ≥ 95%). Transcriptomes of COVID-19 aerocytes, general capillaries and veins were statistically separable from their counterparts in control and IPF lungs (blue dashed boxes); this was not observed for lymphatic, arterial and systemic ECs.

FIGURE 4: PREDICTED ENDOTHELIAL – NON-ENDOTHELIAL CELL INTERACTIONS IN COVID-19 AND IPF LUNGS

A-C, Heatmaps, visualizing the interaction score for the predicted receptor ligand pairs (p ≤ 0.05) within the (A) vascular compartment itself (EC – EC interactions), (B) between ECs and epithelial cells, or (C) between ECs and stromal cells in control, COVID-19 and IPF lungs. Only interactions enriched or

ACCEPTED MANUSCRIPT

reduced in COVID-19 and/or IPF versus control lungs are plotted. In bold indicated and boxed interactions are enriched in COVID-19 or COVID-19 and IPF lungs compared to controls.

FIGURE 5: SYSTEMIC VASCULATURE IN COVID-19 AND IPF LUNGS

A, Representative immunofluorescent images of lung sections from COVID-19 and control subjects, immunostained for CD105 and COL15A1. Hoechst labels nuclei. High magnification (left) and low magnification overview images (right) are shown. Smaller images to the right of larger images are magnifications of the respective boxed areas. Scale bar: 50 µm in high magnification images and their zoom-in areas. Scale bar: 250 µm in low magnification overview images and their zoom-in areas. **B,** Dot plot heatmap of the expression of systemic, capillary and venous EC marker genes. The size and color intensity of each dot represent respectively the percentage of cells within each subcluster expressing the marker gene and the average level of expression of the marker in this subcluster. Color scale: red, high expression; blue, low expression. **C,** SingleR annotation of systemic ECs extracted from the indicated publicly available single cell/nucleus studies, visualized as cluster projections. The top-50 most highly ranking markers of systemic capillary and venous subclusters in our in-house snRNA-seq dataset were used as a reference. **D,** Gene expression heatmap of individual genes involved in ECM production/remodeling and migration, in the indicated cell types and conditions. Genes were selected from GO enrichment analysis, as presented in Table 5. Color scale: red, high expression; blue, low expression. **E,** Principal component analysis (PCA) of pairwise Jaccard similarity coefficients of top-50 marker genes enriched in different EC subclusters extracted from indicated single cell studies. Symbols indicate studies, colors indicate EC subclusters. **F,** UpSet plot of systemic EC-enriched genes across the four different datasets included in the meta-analysis. Black connected dots beneath the graph indicate which studies are intersected. Red bar: 30 intersecting genes commonly enriched in systemic ECs in all studies (false discovery rate (*q* value) < 0.05). **G,** Gene expression heatmap of genes (n=30) commonly enriched in systemic ECs across studies (see red bar in F), in the indicated EC subtypes identified in our snRNA-seq atlas. Color scale: red, high expression; blue, low expression. EC

ACCEPTED MANUSCRIPT

subtypes were pooled into major artery (EC1-3), capillary (cap; EC4-6), vein (EC7-9) and systemic (EC11-12) subgroups. **H,** Violin plots, visualizing the log fold-change distribution of the 30-gene congruent systemic EC signature obtained in (F). Colored dots indicate genes congruently enriched in COVID-19 versus control and/or IPF versus control lungs across all studies included in the analysis; grey dots indicate all other genes in the 30-gene signature.

FIGURE 6: TRANSCRIPTOMIC CHANGES IN THE COVID-19 AND IPF VASCULATURE

Schematic representation of vascular transcriptomic rewiring in COVID-19 and IPF *versus* control lungs. Upper left panel: the vasculature in (lethal) COVID-19 and IPF lungs harbor a gene expression signature suggestive of vascular leakage, decreased barrier integrity, increased ECM deposition, and possible dampened immunity. Upper right panel: EC-centered interactome analysis revealed various routes of EC-microenvironmental cross-talk that could potentially drive the dysfunctional state of the vasculature in COVID-19 and IPF. Lower panel: ECs in lethal COVID-19 and IPF are dominantly enriched for systemic venous and capillary ECs, whereas general (pulmonary) capillary ECs are decreased in abundance. The transcriptomic signature of systemic ECs suggests an involvement in ECM production/deposition, possibly contributing to the overall fibrotic environment in lethal COVID-19 and IPF. ECM: extra-cellular matrix; HSPs: heat shock proteins.

ACCEPTED MANUSCRIPT

Figure 1

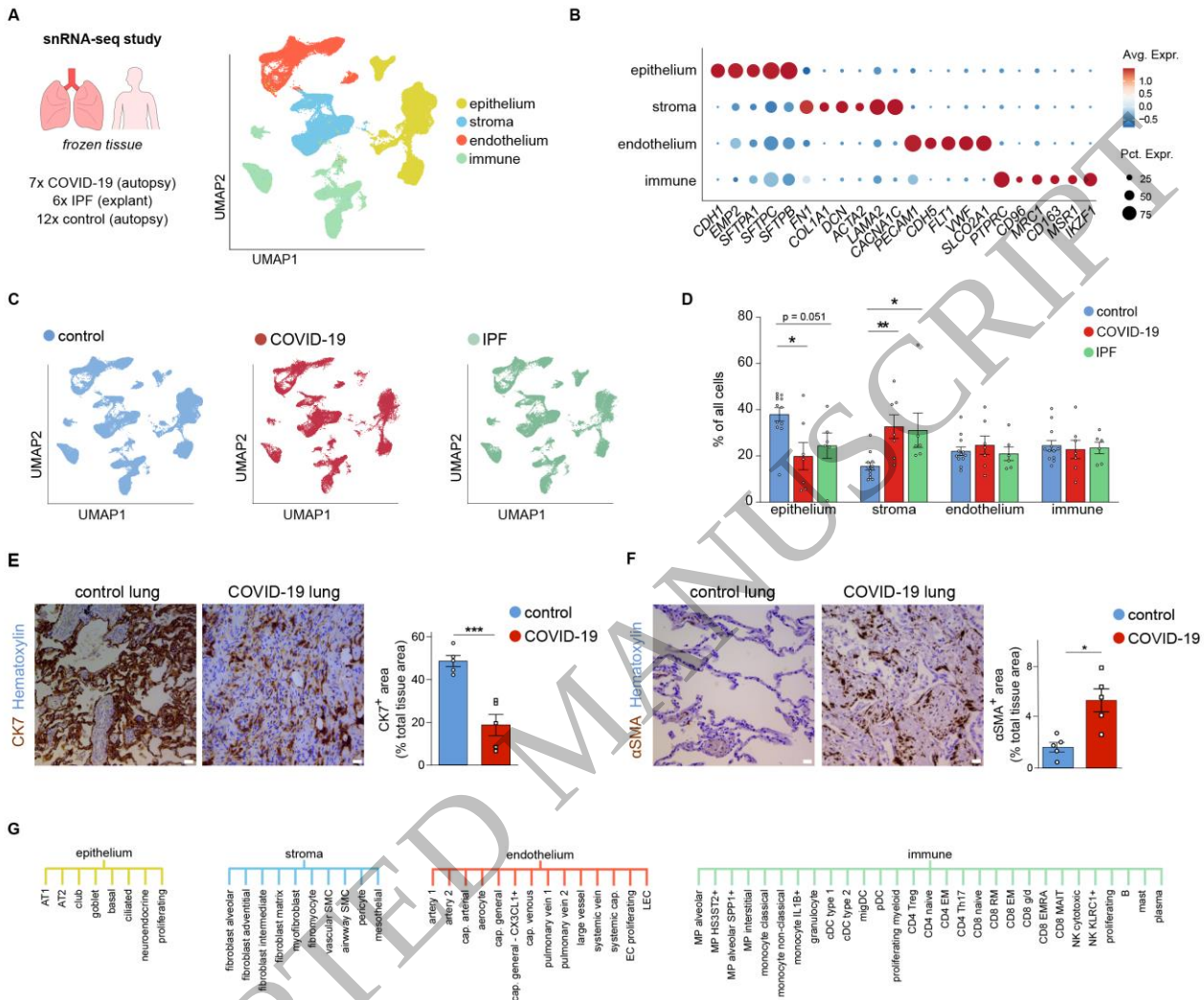

170x144 mm (.17 x DPI)

ACCEPTED MANUSCRIPT

Figure 2

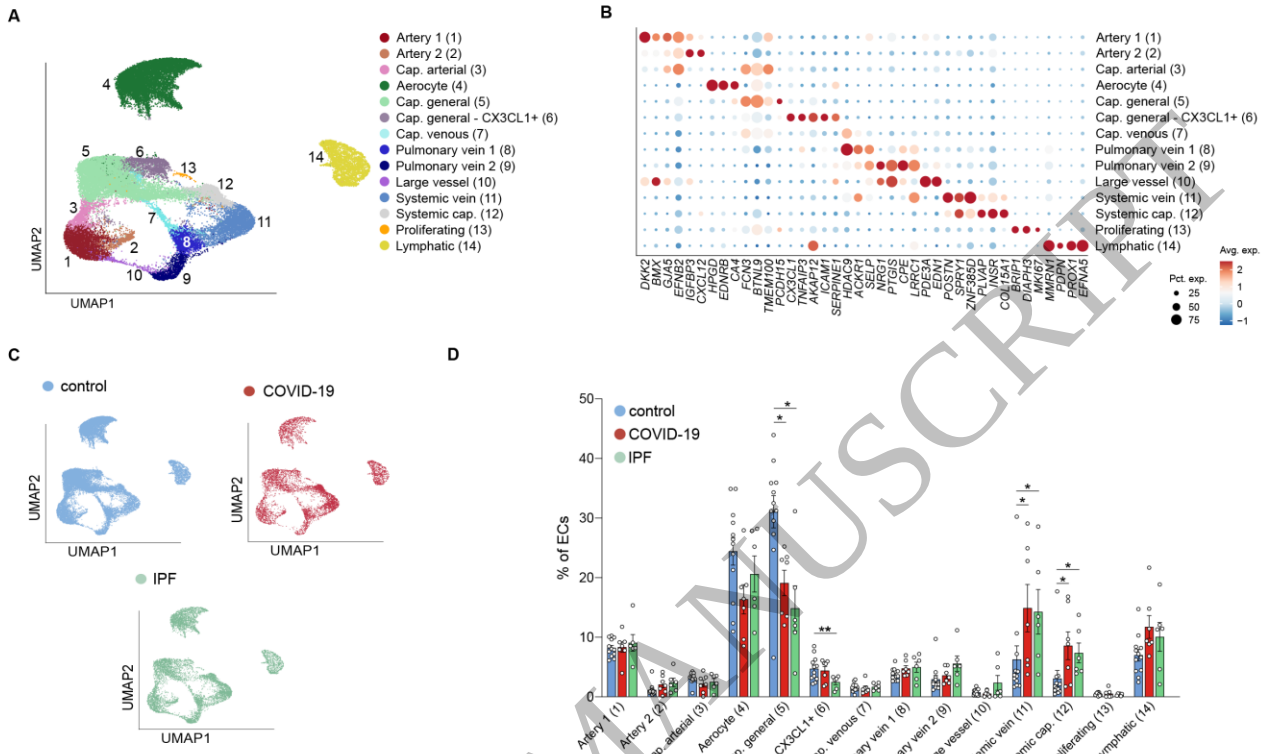

ACCEPTED MANUSCRIPT

170x191 mm (.17 x DPI)

Figure 3

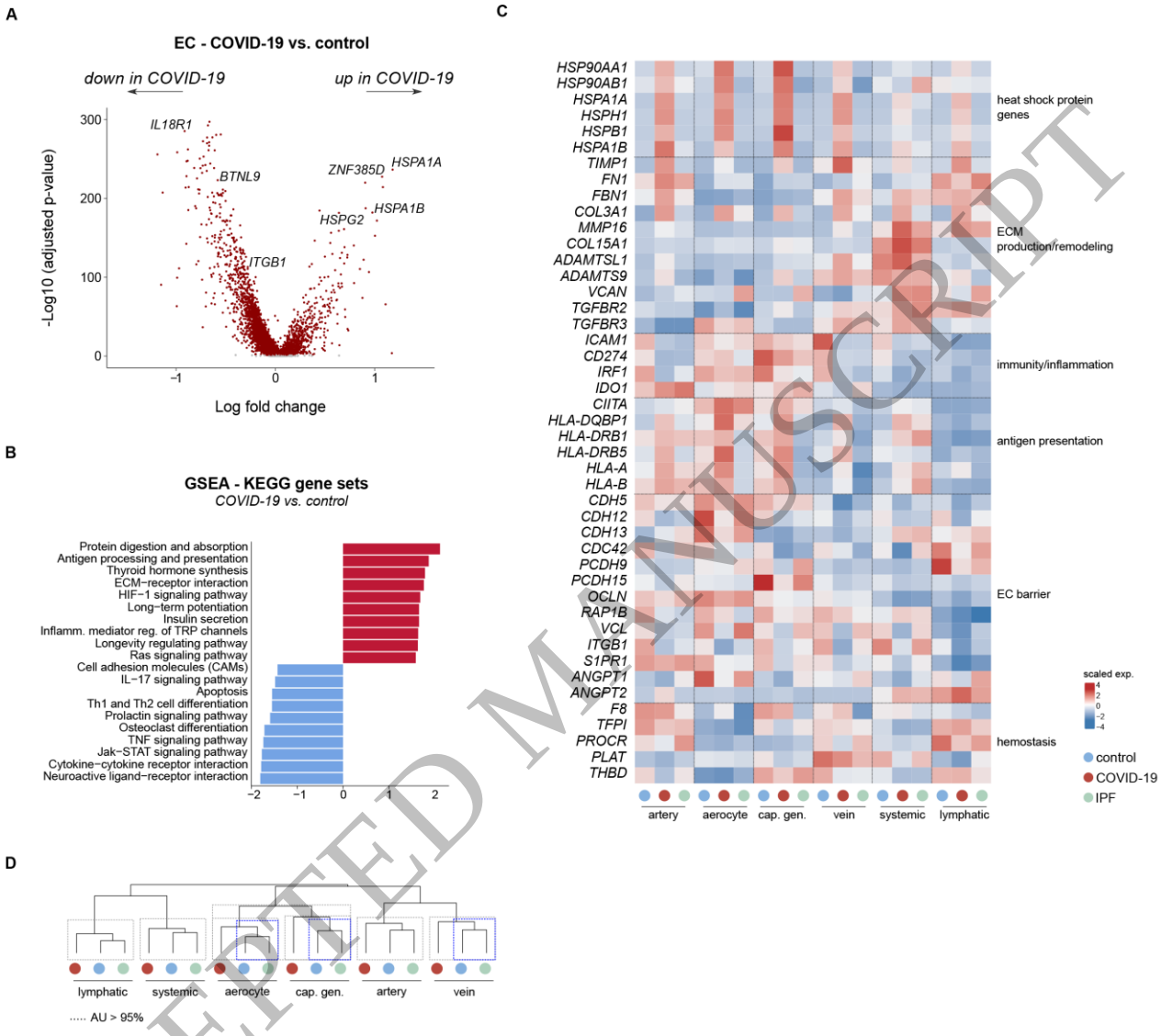

170x153 mm (.17 x DPI)

ACCEPTED MANUSCRIPT

Figure 4

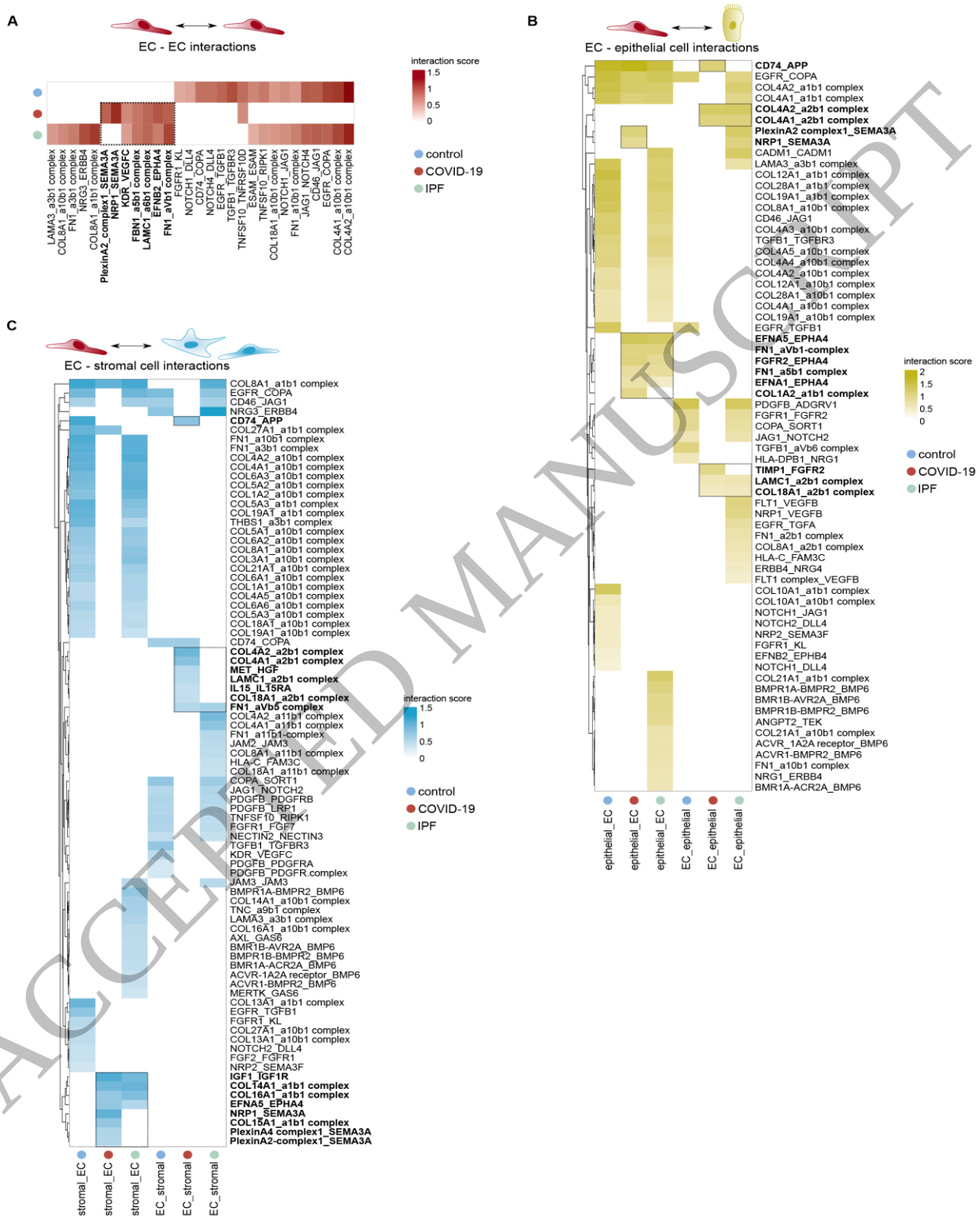

ACCEPTED MANUSCRIPT

170x230 mm (.17 x DPI)

Figure 5

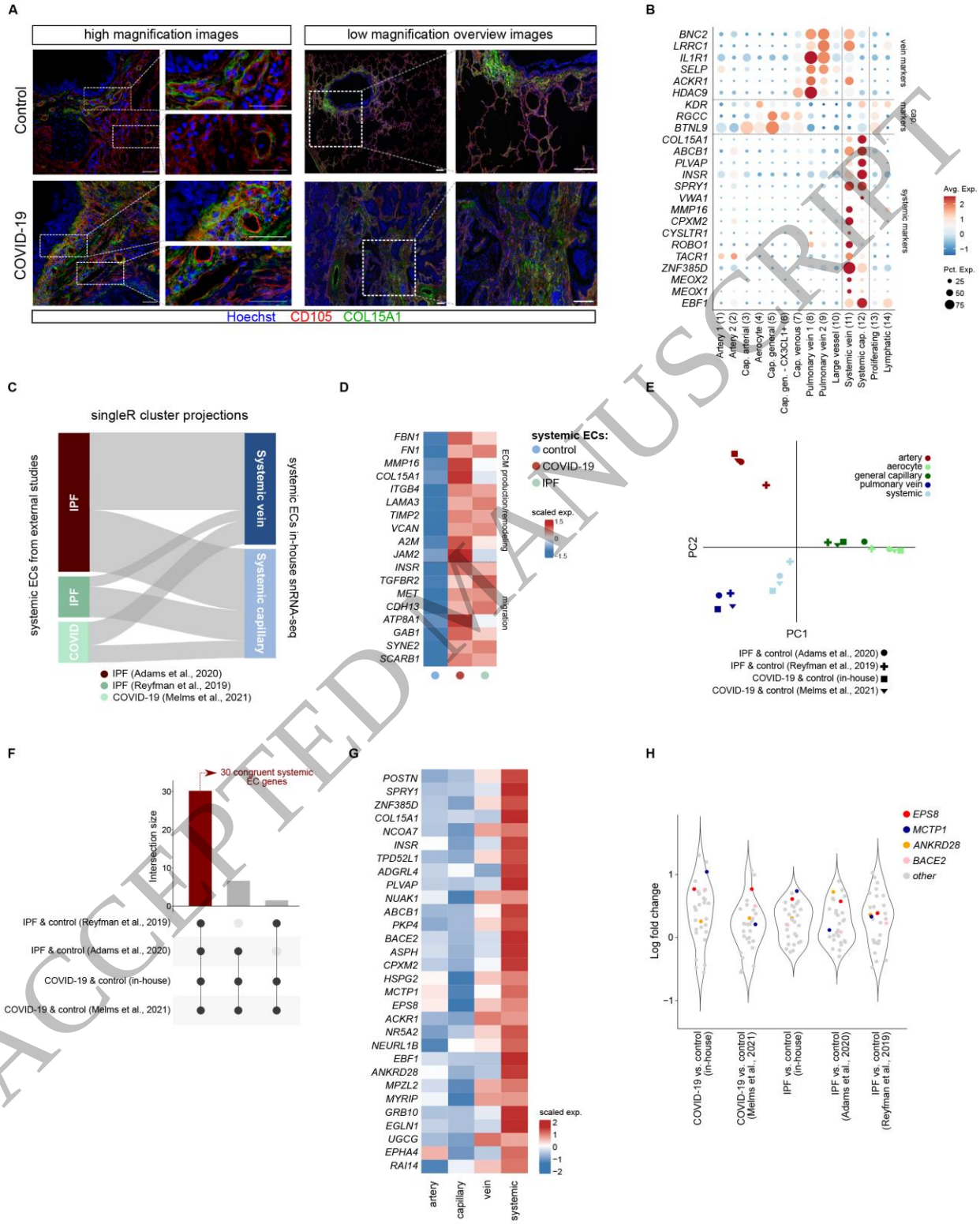

170x219 mm (.17 x DPI)

ACCEPTED MANUSCRIPT

Figure 6

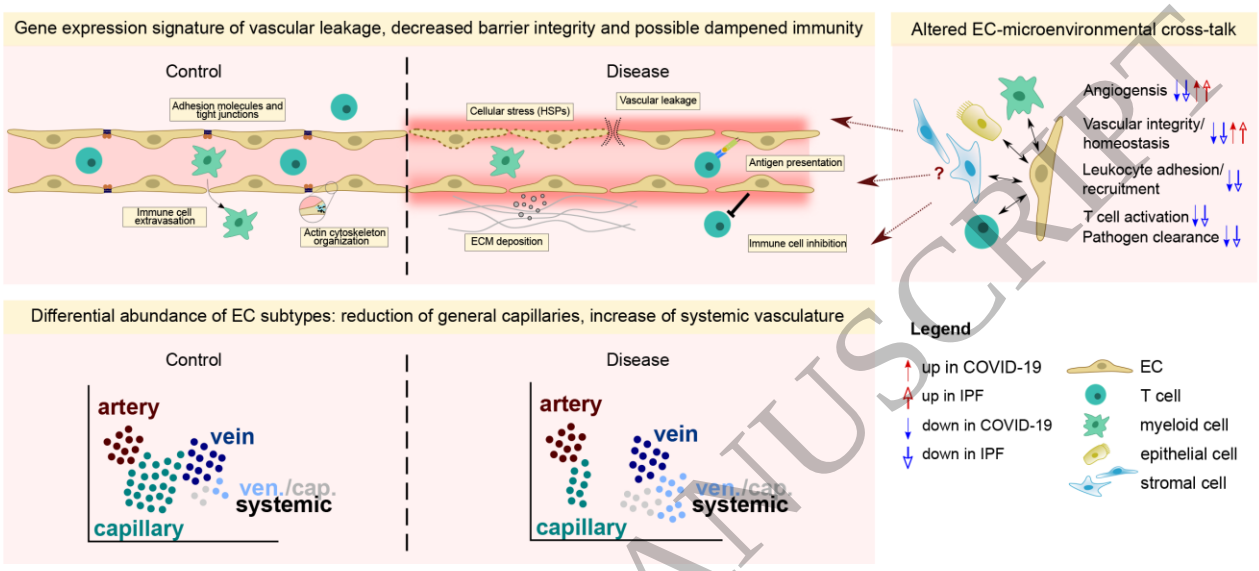

170x86 mm (.17 x DPI)

ACCEPTED MANUSCRIPT